Phenyl-to-Oxo Migration in an Electrophilic Rhenium(VII) Dioxo Complex

Seth N. Brown[1] and James M. Mayer*

Contribution from the Department of Chemistry, Box 351700, University of Washington, Seattle, Washington 98195-1700

Received June 21, 1996[⊗]

Abstract: Reaction of $(HBpz_3)ReO(Ph)(OTf)$ with oxygen atom donors leads to oxidation of the phenyl group [$HBpz_3$ = hydrotris(1-pyrazolyl)borate, OTf = triflate, OSO_2CF_3]. Reaction with Me_2SO gives the adduct $[(HBpz_3)ReO(Ph)(OSMe_2)]OTf$, which undergoes phenyl-to-oxo migration at 25 °C to give the phenoxide complex $[(HBpz_3)ReO(OPh)(OSMe_2)]OTf$ and Me_2S. The Me_2SO adduct readily and reversibly loses Me_2S ($k = 2.9(4)$ s^{-1} at 25 °C) as indicated by isotope exchange reactions and magnetization transfer. The Me_2SO adduct also slowly oxidizes Me_2SO to Me_2SO_2. These reactions all proceed via an intermediate rhenium(VII) dioxo complex, $[(HBpz_3)ReO_2(Ph)]OTf$. This dioxo complex can be observed at low temperature on reaction of $(HBpz_3)ReO(Ph)(OTf)$ with pyridine *N*-oxide. It rearranges at 0 °C by phenyl-to-oxo migration to give phenoxide products and the catecholate complex $(HBpz_3)ReO(O_2C_6H_4)$. The kinetics of this migration have been measured ($\Delta H^{\ddagger} = 14.8(7)$ kcal/mol, $\Delta S^{\ddagger} = -20.5(25)$ eu). From these data and the activation parameters for reactions of $[(HBpz_3)ReO(Ph)(OSMe_2)]OTf$, a detailed free energy surface for the reactions of $[(HBpz_3)ReO_2(Ph)]OTf$ is constructed. The dioxo complex reacts very rapidly with Me_2S (1.7×10^5 M^{-1} s^{-1}) with essentially no enthalpic barrier, consistent with the action of a highly electrophilic oxo ligand. Electrophilicity of the oxo groups is suggested to be a critical factor in facilitating the phenyl-to-oxo migration. A general explanation for the relative ease of various organometallic migration reactions, based on analogies with organic [1,2]-shifts, is presented.

Introduction

The migration of σ-bonded alkyl or aryl groups to terminal oxo ligands in transition metal complexes (eq 1) is a reaction of fundamental interest in high-valent organometallic chemistry. In particular, it offers a potentially useful way of transferring oxidizing equivalents from a metal center to a bound organic ligand. The reaction shown in eq 1 has been invoked for this

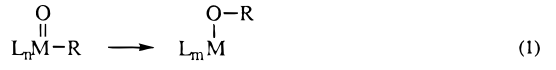

$$L_nM{-}\overset{O}{\overset{\|}{R}} \longrightarrow L_m\overset{O{-}R}{\overset{|}{M}} \qquad (1)$$

purpose in the Sharpless mechanism for *cis*-dihydroxylation of olefins by osmium tetroxide and related species.[2]

Despite its importance there is scant precedent for this transformation. It has been proposed in the reaction of $VOCl_3$ with Ph_2Hg, which gives phenol on addition of H_2SO_4, but neither the starting oxo−aryl complex nor the final aryloxide product were observed directly.[3,4] Analogous migrations to terminal imido[5] or sulfido[6] complexes have also been suggested, again without direct observation of the imido− or sulfido−aryl complexes. Oxo−alkyl complexes are a staple of high-valent organometallic chemistry; hundreds of examples are known, and many show excellent stability.[7] In no case has metal-to-oxo migration been observed in a thermal reaction of an isolable oxo−alkyl or −aryl complex. The reverse reaction, rearrangement of an alkoxide to an oxo−alkyl, is also very rare, with only a single well-documented example.[8,9] Thus, the literature suggests that reaction 1 is not facile in the vast majority of cases.

We recently reported that the rhenium(V) complexes $(HBpz_3)ReO(R)Cl$ [$HBpz_3$ = hydrotris(1-pyrazolyl)borate, R = aryl, ethyl] undergo *photochemical* metal-to-oxo migrations to form rhenium(III) alkoxides.[10] Thermal rearrangements in these systems are once again opposed by large kinetic barriers. Here we describe the generation and observation at low temperature of a rhenium(VII) dioxo−aryl complex, $[(HBpz_3)ReO_2(Ph)]OTf$, which does undergo facile phenyl-to-oxo migration at ambient temperatures. Kinetic and mechanistic data about the migration reaction as well as other oxidation reactions of this rhenium(VII) complex allow the construction of a detailed map of the potential energy surface available to this oxidant and begin to highlight the factors that enable metal-to-oxo migration.

[⊗] Abstract published in *Advance ACS Abstracts,* November 1, 1996.

(1) Current address: Department of Chemistry and Biochemistry, University of Notre Dame, Notre Dame, IN 46556.

(2) (a) Sharpless, K. B.; Teranishi, A. Y.; Bäckvall, J.-E. *J. Am. Chem. Soc.* **1977**, *99*, 3120−3128. (b) Hentges, S. G.; Sharpless, K. B. *J. Am. Chem. Soc.* **1980**, *102*, 4263−4265. (c) Norrby, P. O.; Becker, H.; Sharpless, K. B. *J. Am. Chem. Soc.* **1996**, *118*, 35−42 and references therein. (d) Gable, K. P.; Phan, T. N. *J. Am. Chem. Soc.* **1994**, *116*, 833−839. (e) Jørgensen, K. A.; Schiøtt, B. *Chem. Rev.* **1990**, *90*, 1483−1506.

(3) Reichle, W. T.; Carrick, W. L. *J. Organomet. Chem.* **1970**, *24*, 419.

(4) (a) The purported intermediate in this reaction, $PhVOCl_2$, has been isolated and does not appear to give phenoxides when it decomposes. Thiele, K.-H.; Schumann, W.; Wagner, S.; Brüser, W. *Z. Anorg. Allg. Chem.* **1972**, *390*, 280. (b) For examples of stable $V(O)R_3$ compounds, see: ref 6 and Seidel, W.; Kreisel, G. *Z. Anorg. Allg. Chem.* **1988**, *559*, 118−122. Mowat, W.; Shortland, A.; Yagupsky, G.; Hill, N. J.; Yagupsky, M.; Wilkinson, G. *J. Chem. Soc., Dalton Trans.* **1972**, 533−542.

(5) Nugent, W. A.; Harlow, R. L. *J. Am. Chem. Soc.* **1980**, *102*, 1759.

(6) Vivanco, M.; Ruiz, J.; Floriani, C.; Chiesi-Villa, A.; Rizzoli, C. *Organometallics* **1993**, *12*, 1802−1810.

(7) (a) Bottomley, F.; Sutin, L. *Adv. Organomet. Chem.* **1988**, *28*, 339. (b) Herrmann, W. A. *Angew. Chem., Int. Ed. Engl.* **1988**, *27*, 1297. (c) Spaltenstein, E.; Erikson, T. K. G.; Critchlow, S. C.; Mayer, J. M. *J. Am. Chem. Soc.* **1989**, *111*, 617.

(8) (a) van Asselt, A.; Burger, B. J.; Gibson, V. C.; Bercaw, J. E. *J. Am. Chem. Soc.* **1986**, *108*, 5347. (b) Parkin, G.; Bunel, E.; Burger, B. J.; Trimmer, M. S.; van Asselt, A.; Bercaw, J. E. *J. Mol. Catal.* **1987**, *41*, 21.

(9) Migrations of hydrogen from oxygen to metals has also been observed. See ref 8 and Tahmassebi, S. K.; Conry, R. R.; Mayer, J. M. *J. Am. Chem. Soc.* **1993**, *115*, 7553−7554.

(10) (a) Brown, S. N.; Mayer, J. M. *J. Am. Chem. Soc.* **1994**, *116*, 2219−2220. (b) Brown, S. N.; Mayer, J. M. *Organometallics* **1995**, *14*, 2951−2960.

S0002-7863(96)02087-2 CCC: $12.00

Scheme 1. Preparation of $(HBpz_3)ReO(Ph)OTF$

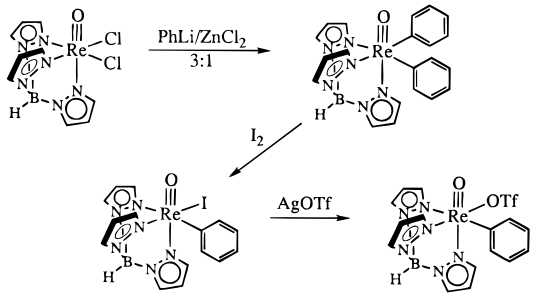

Results

Synthesis and Characterization of Tris(pyrazolyl)borate Rhenium(V) Oxo Triflate Complexes. $(HBpz_3)ReO(Ph)(OTf)$ (OTf = trifluoromethanesulfonate, triflate) is prepared in three steps from the rhenium(V) oxo−dichloride compound $(HBpz_3)ReOCl_2$[11] (Scheme 1). Two phenyl groups are added using the zinc reagent 3:1 PhLi:$ZnCl_2$. One phenyl group in $(HBpz_3)ReO(Ph)_2$ is replaced selectively by iodide on treatment with I_2 (though further reaction to form $(HBpz_3)ReOI_2$ occurs at longer reaction times). $(HBpz_3)ReO(Ph)I$ reacts with 1 equiv of silver triflate to give the blue, diamagnetic, highly moisture-sensitive triflate complex $(HBpz_3)ReO(Ph)(OTf)$. The phenyl chloride complex $(HBpz_3)ReO(Ph)Cl$ also reacts with silver triflate to give the phenyl triflate complex, but this route is less useful because the photochemical preparation of the chloride complex[10a] is difficult to scaleup. The phenyl triflate complex, as expected, shows three inequivalent pyrazoles and a phenyl group in its ^1H and ^{13}C NMR spectra, a strong Re≡O stretch at 976 cm^{-1} in its IR spectrum, and a parent ion in its mass spectrum.

The triflate ligand in $(HBpz_3)ReO(Ph)(OTf)$ is covalently bound, as indicated by observation of a signal in the ^{19}F NMR several ppm downfield of ionic triflate[12] and by infrared data, in particular a band at 1350 cm^{-1} which is diagnostic of covalent η^1-O_3SCF_3 (vs 1280 cm^{-1} in ionic triflate).[13] Confirmation of the presence of covalently bound triflate comes from the crystal structure of $(HBpz_3)ReO(OTf)_2$ synthesized from $(HBpz_3)ReOCl_2$ and AgOTf. Crystal data are summarized in Table 1, and selected bond distances and angles are presented in Table 2. The coordination geometry (Figure 1) is practically superimposable on that displayed by the oxalate complex $(HBpz_3)ReO(C_2O_4)$;[11a] in fact, all of the metal−ligand distances, except those of the pyrazoles *trans* to the oxo, are the same (within experimental error) in the two structures. This is remarkable in that metal−triflate distances are generally observed to be significantly elongated relative to other metal−oxygen distances in related complexes.[13] The highly covalent nature of the rhenium−triflate linkage is indicated both by the short Re−O bonds (2.014 Å av) and by the lengthening of the bond between the sulfur and the oxygen bound to rhenium (1.504 vs 1.400 Å for the sulfonyl oxygens).

Synthesis and Reactivity of $[(HBpz_3)ReO(Ph)(OSMe_2)]$-OTf. Despite being bound covalently, the triflate in $(HBpz_3)ReO(Ph)(OTf)$ is readily displaced by a variety of other ligands. For example, the phenyl triflate complex reacts immediately with dimethyl sulfoxide (Me_2SO, DMSO) in CH_2Cl_2 to form the adduct $[(HBpz_3)ReO(Ph)(OSMe_2)]OTf$ (eq 2). The binding constant of Me_2SO to the triflate complex is too large to be measured reliably by NMR. No unreacted $(HBpz_3)ReO(Ph)(OTf)$ is apparent in the presence of even a slight excess of Me_2SO. In contrast, Me_2S binds weakly to rhenium in CD_2Cl_2, forming an adduct $[(HBpz_3)ReO(Ph)(SMe_2)]OTf$ in equilibrium with the covalent triflate complex. The concentrations of these species

Table 1. Crystal Data for $(HBpz_3)ReO(O_3SCF_3)_2\cdot C_6D_6$

formula	$C_{17}H_{10}D_6BF_6N_6O_7ReS_2$
fw	797.5
crystal size, mm	0.20 × 0.25 × 0.35
space group	$P2_1/c$
λ, Å	Mo Kα, 0.71073
T, °C	25
a, Å	10.510(2)
b, Å	17.129(2)
c, Å	15.600(4)
β, deg	106.71(2)
Z	4
V, Å^3	2690.1(14)
ρ_{calc}, g cm^{-3}	1.969
μ, cm^{-1}	47.63
transmission coeffecient	0.62−0.99
reflections measured	5727
unique reflections	4725
obsd reflections ($F > 4\sigma(F)$)	3834
refined parameters	362
R_{av}	0.0275
R	0.0476
R_w	0.0657
goodness of fit	1.22

Table 2. Selected Bond Distances (Å) and Angles (deg) in $(HBpz_3)ReO(O_3SCF_3)_2\cdot C_6D_6$

Re−O(1)	1.667(9)	Re−N(12)	2.065(10)
Re−O(11)	2.016(8)	Re−N(22)	2.070(11)
Re−O(21)	2.011(10)	Re−N(32)	2.213(9)
S(1)−O(11)	1.494(10)	S(2)−O(21)	1.515(9)
S(1)−O(12)	1.380(13)	S(2)−O(22)	1.424(11)
S(1)−O(13)	1.398(13)	S(2)−O(23)	1.399(11)
O(1)−Re−O(11)	102.7(4)	O(11)−Re−O(21)	83.2(4)
O(1)−Re−O(21)	103.4(4)	O(11)−Re−N(12)	166.2(3)
O(1)−Re−N(12)	90.7(4)	O(21)−Re−N(22)	161.0(4)
O(1)−Re−N(22)	94.0(4)	Re−O(11)−S(1)	139.3(6)
O(1)−Re−N(32)	169.3(5)	Re−O(21)−S(2)	134.4(6)
N(12)−Re−N(22)	90.5(4)		

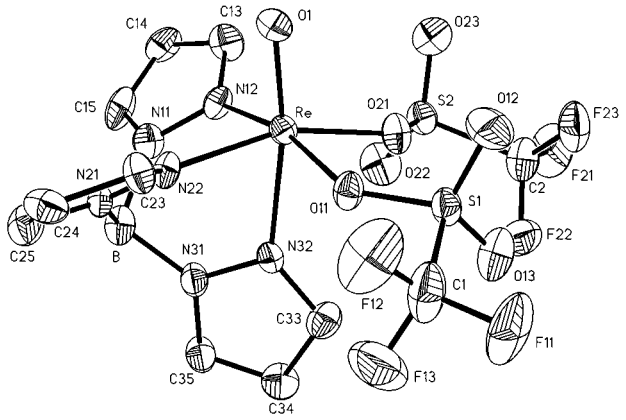

Figure 1. ORTEP drawing of $(HBpz_3)ReO(OTf)_2$.

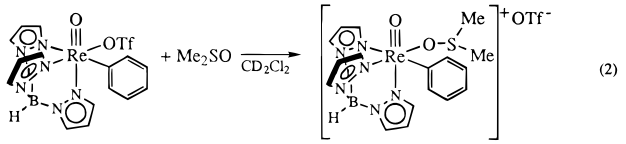

(2)

(11) (a) Brown, S. N.; Mayer, J. M. *Inorg. Chem.* **1992**, *31*, 4091−4100. (b) Abrams, M. J.; Davison, A.; Jones, A. G. *Inorg. Chim. Acta* **1984**, *82*, 125. (c) Degnan, I. A.; Behm, J.; Cook, M. R.; Herrmann, W. A. *Inorg. Chem.* **1991**, *30*, 2165.

(12) Conry, R. R.; Mayer, J. M. *Organometallics* **1993**, *12*, 3179−3186.

(13) Lawrance, G. A. *Chem. Rev.* **1986**, *86*, 17−33.

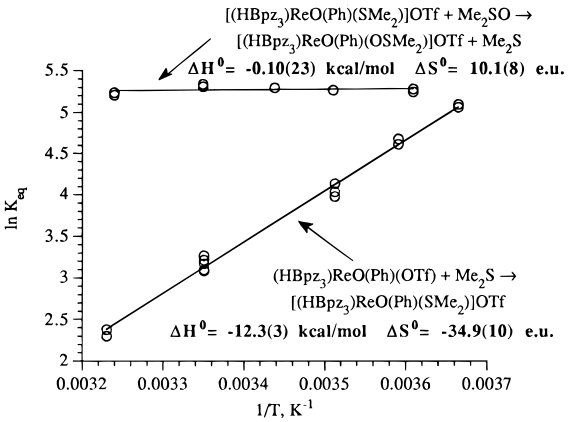

Figure 2. Van't Hoff plots of binding of Me_2S and Me_2SO to $(HBpz_3)$-ReO(Ph)(OTf).

can be measured by NMR (eq 3a). If present in large excess,

$$LReO(Ph)(OTf) + Me_2S \rightleftarrows [LReO(Ph)(SMe_2)]OTf \qquad K = 23.8(17)\ M^{-1} \quad (3a)$$

$$[LReO(Ph)(SMe_2)]OTf + Me_2SO \rightleftarrows [LReO(Ph)(OSMe_2)]OTf + Me_2S \qquad K = 205(5) \quad (3b)$$

$$LReO(Ph)(OTf) + Me_2SO \rightleftarrows [LReO(Ph)(OSMe_2)]OTf \qquad K = 4.9(4) \times 10^3\ M^{-1} \quad (3c)$$

Me_2S can also compete with Me_2SO for the rhenium center (eq 3b). From these two reactions, a binding constant for Me_2SO to the rhenium triflate complex may be calculated (eq 3c, $T =$ 298 K and L = $HBpz_3$ in all three equations). Measurements of the equilibrium in eq 3a made at concentrations of rhenium from 6.5 to 17 mM in the presence of a roughly 10-fold excess of Me_2S show a concentration dependence that indicates that the adduct $[(HBpz_3)ReO(Ph)(SMe_2)]OTf$ is tightly ion-paired in methylene chloride. Other adducts should be of similar size and are also expected to form tight ion pairs.

The equilibrium constants for eqs 3a and 3b were determined as a function of temperature in the range of 4−37 °C. Van't Hoff plots of the data are displayed in Figure 2. The displacement of Me_2S from rhenium by Me_2SO is quite favorable (eq 3b) but is practically temperature-independent, indicating it is entirely driven by entropy ($\Delta H° = -0.1(2)$ kcal/mol, $\Delta S° = +10.1(8)$ eu). This may be due to strong solvation of the very polar Me_2SO by the methylene chloride, giving it a relatively favorable enthalpy and unfavorable entropy of solvation. Binding the oxygen of DMSO to the oxophilic rhenium(V) center would offset the unfavorable loss of solvation enthalpy. Since the rhenium sulfoxide and sulfide adducts should be solvated virtually identically, replacing polar Me_2SO in solution with nonpolar Me_2S should result in a net gain in entropy. Addition of the thermodynamic parameters for reactions 3a and 3b gives the enthalpy and entropy for binding Me_2SO to $(HBpz_3)ReO(Ph)(OTf)$: $\Delta H° = -12.4(4)$ kcal/mol, $\Delta S° = -24.8(13)$ eu, $\Delta G°_{298} = -5.0(6)$ kcal/mol.

The ^1H NMR spectrum of the blue DMSO adduct $[(HBpz_3)$-$ReO(Ph)(OSMe_2)]OTf$ in CD_2Cl_2 displays resonances due to three inequivalent pyrazoles, consistent with the lack of symmetry in the molecule. Also present are the expected three resonances for the phenyl group and two singlets of intensity 3 H at δ 3.12 and 3.23 ppm. These two peaks are absent when the complex is made from $(CD_3)_2SO$ and are ascribed to the two diastereotopic methyl groups of a single bound Me_2SO. Since these resonances are more than 0.5 ppm downfield of free Me_2SO and do not shift in the presence of excess ligand, sulfoxide exchange is slow on the NMR time scale.

The IR spectrum of the dimethyl sulfoxide adduct, obtained in chloroform in the presence of excess Me_2SO and Me_2S, shows the usual bands due to the tris(pyrazolyl)borate ligand, a normal Re≡O stretch ($\nu = 985$ cm^{-1}), and bands due to ionic triflate (1276, 1164, and 1030 cm^{-1}). In addition, there is a strong broad band at 858 cm^{-1} due to coordinated S−O, whose assignment is confirmed by synthesis of the complex from ^{18}O-enriched Me_2SO ($\nu_{S-^{18}O} = 826$ cm^{-1}, calcd 826 cm^{-1} for a diatomic S−O stretch). (The oxo group is also enriched by this procedure, for reasons which will become apparent below, and shifts to 948 cm^{-1} [calcd 933 cm^{-1}].) Since the S−O stretch decreases in frequency in O-bound sulfoxide complexes and increases in frequency in S-bound complexes,[14] the IR spectra confirm that the sulfoxide oxygen is bound to rhenium ($\nu_{SO} = 1055$ cm^{-1} for free Me_2SO[15]). Typical S−O stretches in O-bound DMSO complexes are in the 900−1000 cm^{-1} range; the frequency observed here is at least 20 cm^{-1} lower than that of any sulfoxide complex of which we are aware.[15−18] This unprecedentedly low sulfur−oxygen stretching frequency indicates significant sulfur−oxygen bond weakening on coordination to the rhenium center.

Weakening of the sulfur−oxygen bond is reflected in the reactivity of $[(HBpz_3)ReO(Ph)(OSMe_2)]OTf$: the Me_2S fragment of the coordinated dimethyl sulfoxide undergoes facile exchange with free Me_2S. This was demonstrated by condensing $(CH_3)_2S$ onto frozen CD_2Cl_2 solutions of $[(HBpz_3)ReO$-$(Ph)(OS[CD_3]_2)]OTf$, prepared by adding excess $(CD_3)_2SO$ to the triflate complex. ^1H NMR spectra of samples placed directly in the probe of the NMR spectrometer at −78 °C show resonances for the sulfoxide complex in the pyrazole region of the spectrum, but only those due to free $(CH_3)_2S$ in the methyl region. When the sample was warmed to −50 °C, the two singlets due to bound $OS(CH_3)_2$ appear and slowly grow in intensity, eventually achieving a constant value which depends on the ratio of Me_2S to rhenium complex. At −50 °C, free protio $(CH_3)_2SO$ does not appear at a significant rate. Only at higher temperatures is there any exchange of excess free $(CD_3)_2$-SO with bound $(CH_3)_2SO$. This indicates that the exchange between dimethyl sulfide and bound dimethyl sulfoxide cannot involve free Me_2SO.

The incorporation of protium into bound dimethyl sulfoxide obeys the first-order approach to equilibrium kinetics (Figure 3). Indeed, it must do so regardless of the mechanism of the reaction, since the concentrations of all chemical species—and hence the rates of all chemical reactions—remain constant,[19] with only the distribution of deuterium shifting with time. It can be shown (Supporting Information) that the observed rate constant for the isotope exchange is given by eq 4, where R is the rate

$$k_{obs} = R\left(\frac{1}{[Re]} + \frac{1}{[Me_2S]}\right) \qquad (4)$$

of the chemical process that exchanges free and bound Me_2S. As shown in Figure 4, the variation of k_{obs} with rhenium and

(14) Nakamoto, K. *Infrared and Raman Spectra of Inorganic and Coordination Compounds*, 3rd ed.; Wiley: New York, 1978; 344−346.
(15) Reynolds, W. L. *Prog. Inorg. Chem.* **1970**, *12*, 1−99.
(16) Davies, J. A. *Adv. Inorg. Chem. Radiochem.* **1981**, *24*, 115−187. Furukawa, N.; Fujihara, H. In *The Chemistry of Sulphones and Sulphoxides*; Patai, S., Rappoport, Z., Stirling, C. J. M., Eds.; John Wiley and Sons: New York, 1988; 541−581.
(17) The closely related complex $[(HBpz_3)ReO(OEt)(OSMe_2)]OTf$[18] has an S−O stretching frequency of 872 cm^{-1}.
(18) DuMez, D. D.; Mayer, J. M. *Inorg. Chem.* **1995**, *34*, 6396−6401.
(19) This neglects small changes in rate due to secondary isotope effects.

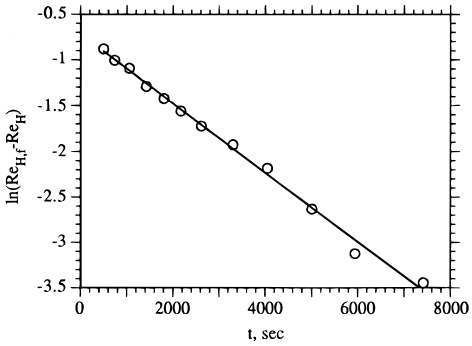

Figure 3. First-order plot of the incorporation of protium into [(HBpz$_3$)ReO(Ph)(OS[CD$_3$]$_2$)]OTf from (CH$_3$)$_2$S at 223 K.

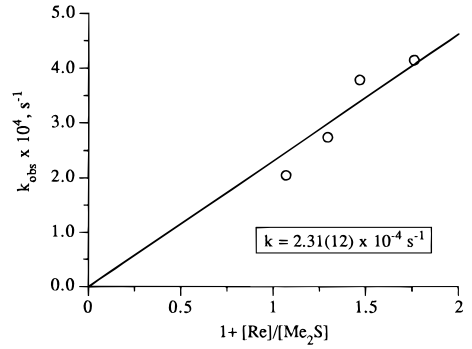

Figure 4. Plot of k_{obs} vs (1 + [Re]/[Me$_2$S]) for isotope exchange between [(HBpz$_3$)ReO(Ph)(OS(CD$_3$)$_2$)]OTf and (CH$_3$)$_2$S at 223 K.

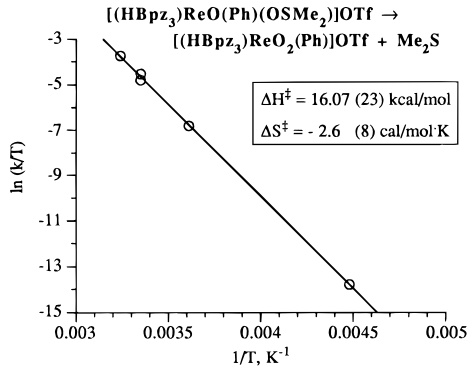

Figure 5. Eyring plot for [(HBpz$_3$)ReO(Ph)(OSMe$_2$)]OTf → [(HBpz$_3$)ReO$_2$(Ph)]OTf + Me$_2$S.

dimethyl sulfide concentration gives a satisfactory fit to eq 4 with $R = k$[Re] and $k = 2.31(12) \times 10^{-4}$ s^{-1} at 223 K. In particular, increasing the [Me$_2$S] at fixed rhenium concentration *decreases* the k_{obs}, establishing that the exchange process is zero order in Me$_2$S.

Exchange of the dimethylsulfur unit between [(HBpz$_3$)ReO(Ph)(OSMe$_2$)]OTf and free Me$_2$S can also be observed at room temperature by magnetization transfer in the ^{1}H NMR. Selective inversion of the signal for free Me$_2$S is followed by transfer of that magnetization to the diastereotopic methyl singlets of the ReOS(C*H*$_3$)$_2$. From the time course of the magnetization transfer, a rate constant may be derived ($k = 2.9$ (4) s^{-1} at 298 K). Figure 5 shows an Eyring plot constructed from rate constants measured by magnetization transfer at several temperatures close to ambient as well as the rate constant measured by isotopic exchange at 223 K. The excellent agreement of the low-temperature measurement with that extrapolated from the magnetization-transfer experiments confirms that the two observations share a common mechanism, and the 85 °C range permits an unusually precise measurement of the activation parameters of the reaction, $\Delta H^{\ddagger} = 16.1(2)$ kcal/mol and $\Delta S^{\ddagger} = -2.6(8)$ eu. The substantial enthalpy of activation and the small entropy of activation suggest a dissociative mechanism, consistent with the reaction being zero order in Me$_2$S. All the data strongly point to exchange occurring via rate-limiting loss of Me$_2$S from the Me$_2$SO adduct to form the dioxo complex [(HBpz$_3$)ReO$_2$(Ph)]OTf, followed by rebinding of Me$_2$S (eq 5).

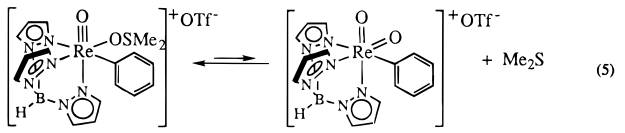

(5)

Dissociation of Me$_2$S can also be monitored by magnetization transfer among the pyrazole ligands, because eq 5 should equilibrate two of the pyrazole ligands. Selective inversion of the triplet corresponding to the pyrazole 4-H *trans* to the oxo group in [(HBpz$_3$)ReO(Ph)(OSMe$_2$)]OTf (δ 6.11 ppm in CD$_2$Cl$_2$) does lead to transfer of magnetization, but to *both* of the other pyrazole triplets (δ 6.48 and 6.66 ppm) at an equal rate. It is surprising that the third pyrazole is affected, as this should remain *trans* to the phenyl group. The pyrazole magnetization transfer is the same process as Re−O*SMe*$_2$ exchange because the two occur with the same rate constant, within experimental error. These data suggest that [(HBpz$_3$)ReO$_2$(Ph)]OTf, the product of Me$_2$S dissociation, is fluxional at room temperature.

In addition to the rapid degenerate process of exchanging its Me$_2$S group with free Me$_2$S, [(HBpz$_3$)ReO(Ph)(OSMe$_2$)]OTf undergoes two slower processes that effect net chemical change. Oxidation of the phenyl group to phenoxide occurs, forming a new rhenium complex, [(HBpz$_3$)ReO(OPh)(OSMe$_2$)]OTf, in about 70% yield based on the amount of rhenium phenyl complex consumed (eq 6). (The reaction does not go to

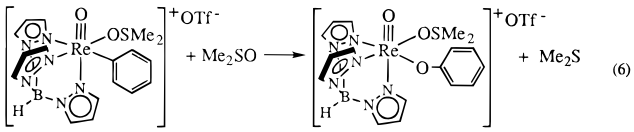

(6)

completion for reasons discussed below.) Formation of the phenoxide has been confirmed in two ways. First, [(HBpz$_3$)ReO(OPh)(OSMe$_2$)]OTf can be prepared independently by addition of Me$_2$SO to (HBpz$_3$)ReO(OPh)(OTf). The triflate complex is in turn formed from the bis(phenoxide) complex (HBpz$_3$)ReO(OPh)$_2$ by selective cleavage of one phenoxide group by trimethylsilyl triflate (eq 7), as observed for related

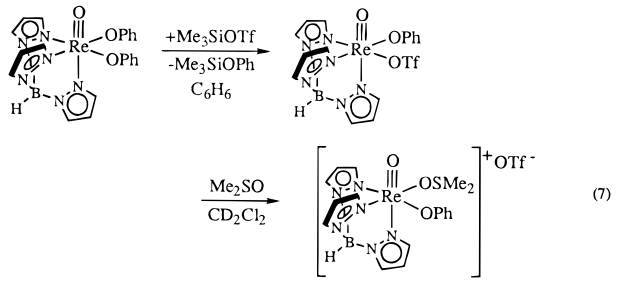

(7)

bis(alkoxide) complexes.[18] Second, addition of tetramethylammonium chloride to the reaction mixture of (HBpz$_3$)ReO(Ph)(OTf) and Me$_2$SO yields the known[10b] neutral complex (HBpz$_3$)ReO(OPh)(Cl).

In addition to undergoing phenyl to phenoxide conversion, [(HBpz$_3$)ReO(Ph)(OSMe$_2$)]OTf catalyzes the disproportionation of dimethyl sulfoxide, leading to the formation of both dimethyl

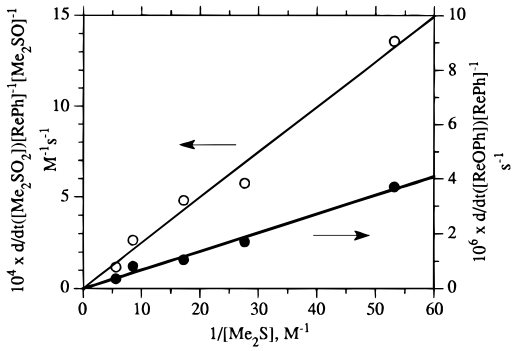

Figure 6. Inhibition of reactions of [(HBpz$_3$)ReO(Ph)(OSMe$_2$)]OTf by Me$_2$S. Closed circles indicate initial rates of phenyl oxidation (eq 6), corrected for rhenium concentration; open circles indicate initial rates of oxidation of Me$_2$SO to Me$_2$SO$_2$ (eq 8), corrected for rhenium and Me$_2$SO concentration.

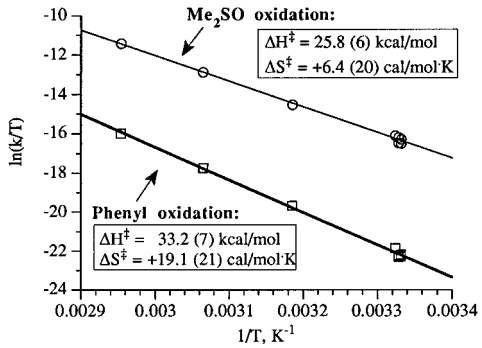

Figure 7. Eyring plots for eq 6 (open squares) and eq 8 (open circles).

sulfide and dimethyl sulfone (eq 8). This represents oxygen

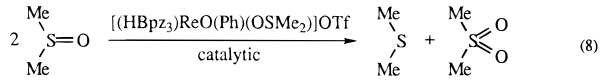

(8)

atom transfer from Me$_2$SO to another molecule of Me$_2$SO. Oxygen atom transfer is not limited to dimethyl sulfoxide as the reductant; for example, triphenylphosphine is rapidly oxidized to triphenylphosphine oxide by Me$_2$SO in the presence of catalytic amounts of (HBpz$_3$)ReO(Ph)(OTf).

The processes of eqs 6 and 8 are both strongly inhibited by free dimethyl sulfide. Because both reactions produce Me$_2$S, and because reaction 8 uses up the free Me$_2$SO (and eventually the bound sulfoxide) before reaction 6 can go to completion, the time course of reactions of [(HBpz$_3$)ReO(Ph)(OSMe$_2$)]OTf is complex. However, kinetics can be measured reliably using initial rates (over the first 10% or so of reaction) in the presence of a substantial excess of Me$_2$S. Rates of reaction were determined by NMR; the rate for reaction 6 was determined from the growth of the diastereotopic methyl peaks due to [(HBpz$_3$)ReO(OPh)(OS*Me*$_2$)]OTf and the rate for reaction 8 from the growth of the Me$_2$SO$_2$ signal. From reactions conducted at different concentrations of rhenium complex and of Me$_2$SO, it is apparent that both reactions are first order in rhenium and that the rate of eq 8 is proportional to [Me$_2$SO] while that of eq 6 is independent of Me$_2$SO concentration. The effect of added dimethyl sulfide on the reactions can be seen from Figure 6: Both reactions are inverse first order in Me$_2$S. This indicates that preequilibrium loss of Me$_2$S from [(HBpz$_3$)-ReO(OPh)(OSMe$_2$)]OTf precedes the rate-limiting step in both phenyl oxidation and sulfoxide oxidation. The temperature dependence of the two reactions (Figure 7) bolsters this conclusion, since the positive entropies of activation (+19.1 eu for phenyl oxidation, +6.4 eu for Me$_2$SO oxidation) are most

Scheme 2. Reactions of [(HBpz$_3$)ReO(Ph)(OSMe$_2$)]OTf

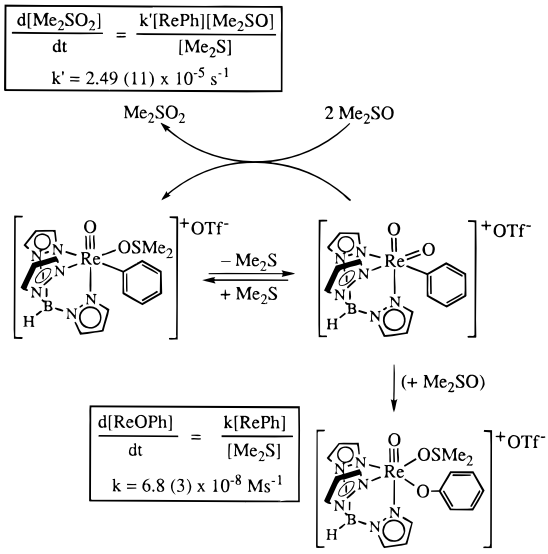

consistent with generation of an entire separate particle before the transition state. (The $\Delta S^{\ddagger}$ for DMSO oxidation is expected to be less positive since a bimolecular step follows Me$_2$S loss.) Loss of Me$_2$S from [(HBpz$_3$)ReO(OPh)(OSMe$_2$)]OTf forms [(HBpz$_3$)ReO$_2$(Ph)]OTf (see above), implicating the rhenium-(VII) dioxo complex as an intermediate common to catalytic sulfoxide disproportionation and to phenyl oxidation (Scheme 2).

Reaction of (HBpz$_3$)ReO(Ph)(OTf) with Pyridine *N*-Oxide; Direct Observation of [(HBpz$_3$)ReO$_2$(Ph)]OTf. The rhenium-(VII) dioxo complex [(HBpz$_3$)ReO$_2$(Ph)]OTf is accessible from [(HBpz$_3$)ReO(Ph)(OSMe$_2$)]OTf, but the equilibrium favors rhenium(V) over rhenium(VII). The more powerful oxygen atom donor pyridine *N*-oxide (py-O) reacts immediately with (HBpz$_3$)ReO(Ph)(OTf) at −78 °C in dichloromethane to give a deep orange solution. The ^{1}H NMR spectrum of the reaction mixture at this temperature shows free pyridine, a small amount of (HBpz$_3$)ReO$_3$, and a rhenium-containing intermediate. Roughly half of the rhenium does not appear at all in the NMR (based on integration vs an internal toluene standard), presumably because it has reacted to form paramagnetic NMR-silent materials. The amount of unobserved rhenium material does not appear to be affected by the quantity of oxidant added. The observed intermediate exhibits broad resonances in the ^{1}H NMR for both the pyrazole and phenyl ligands, so that only limited structural information is available. The chemical shifts are normal, indicating that this species is diamagnetic. The relatively small number of resonances observed is consistent with a complex containing a plane of symmetry. As the temperature is raised the spectrum changes reversibly, with most resonances broadening and with the two peaks at ca. 6.7 ppm coalescing at ∼215 K. This suggests that the intermediate is fluxional. The NMR spectra and the chemical trapping presented below suggest assignment of the intermediate as the dioxo−phenyl complex [(HBpz$_3$)ReO$_2$(Ph)]OTf (eq 9). Its

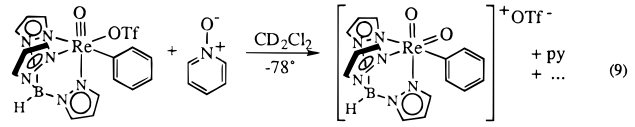

(9)

fluxionality is consistent with the magnetization transfer among the pyrazole ligands discussed above.

Addition of Me$_2$S at −78 °C to the intermediate—the deep orange solution generated from (HBpz$_3$)ReO(Ph)(OTf) and

C_5H_5NO at this temperature— immediately bleaches the solution to light green. NMR spectra at this temperature show that the broad lines are absent and have been replaced by signals due to [(HBpz$_3$)ReO(Ph)(OSMe$_2$)]OTf (eq 10). The DMSO adduct

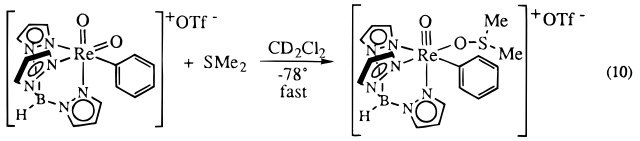

(10)

is stable at −78 °C, though at −50 °C the pyridine formed from reduction of pyridine *N*-oxide slowly displaces the Me_2SO to form [(HBpz$_3$)ReO(Ph)(py)]OTf.

The orange solution of [(HBpz$_3$)ReO$_2$(Ph)]OTf is stable for days if kept in a dry ice−acetone bath in a sealed NMR tube. However, if solutions are allowed to warm to ca. 0 °C, the broad signals of the dioxo complex slowly diminish in intensity and three products of phenyl oxidation are observed: the phenoxy−pyridine adduct [(HBpz$_3$)ReO(OPh)(py)]OTf, the known phenoxy−chloride complex (HBpz$_3$)ReO(OPh)(Cl),[10b] and the rhenium(V) catecholate complex (HBpz$_3$)ReO($O_2C_6H_4$) (eq 11).

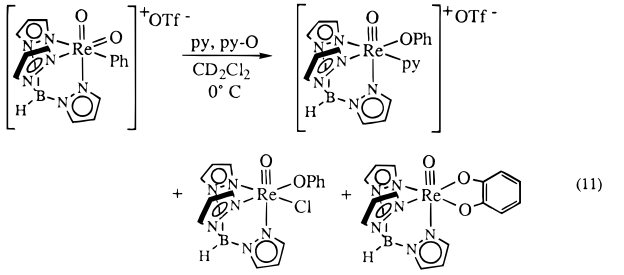

(11)

Some of the trioxo complex (HBpz$_3$)ReO$_3$ is also formed. The origin of the chloride in (HBpz$_3$)ReO(OPh)Cl is uncertain, but it presumably comes from degradation of the CD_2Cl_2 solvent during the reaction; note that isolated (HBpz$_3$)ReO(OPh)(OTf) does not abstract chloride from dichloromethane.

The identities of the oxidation products in eq 11 have been confirmed by independent syntheses. The catechol complex is prepared from (HBpz$_3$)ReOCl$_2$ and catechol/triethylamine, and the phenoxy−pyridine complex is formed on addition of pyridine to (HBpz$_3$)ReO(OPh)(OTf) (compare formation of the DMSO adduct, eq 7). Together the three oxidation products shown in eq 11 account for essentially all of the dioxo intermediate initially present (>90%). Their relative amounts depend on the amount of excess pyridine *N*-oxide present in solution. The catecholate complex (HBpz$_3$)ReO($O_2C_6H_4$) is the favored product in the presence of a large excess of C_5H_5NO, while the two phenoxide products become increasingly prevalent when there is a smaller amount of oxidant. Using about 3 equiv of pyridine *N*-oxide, the distribution of the products is ca. 1:1:5 phenoxy−pyridine:phenoxy−chloride:catecholate. When the oxidation is conducted at room temperature with an excess of pyridine *N*-oxide, no phenoxide products are observed at all. The absolute yield of catecholate complex under these conditions is 35%, based on the starting triflate, or about 70% based on the dioxo formed. If less than 1 equiv of pyridine *N*-oxide is used and the reaction is conducted at low temperature, only a trace amount of catecholate is formed.

The relative yield of products depends on the amount of excess oxidant, but the rate of disappearance of the dioxo−phenyl complex does not. Therefore, the three products appear to be derived from [(HBpz$_3$)ReO$_2$(Ph)]OTf via a common intermediate, likely the phenoxide complex (HBpz$_3$)ReO(OPh)-(OTf). As observed in independent reactions of isolated

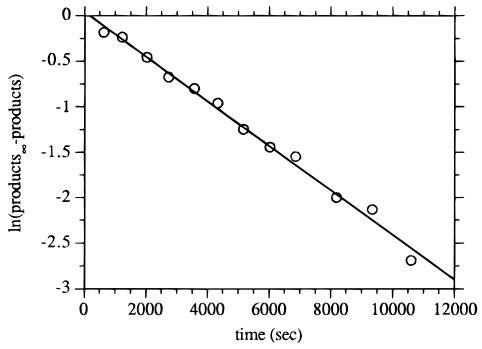

Figure 8. First-order plot for phenyl oxidation in [(HBpz$_3$)ReO$_2$(Ph)]OTf (CD_2Cl_2, 272 K).

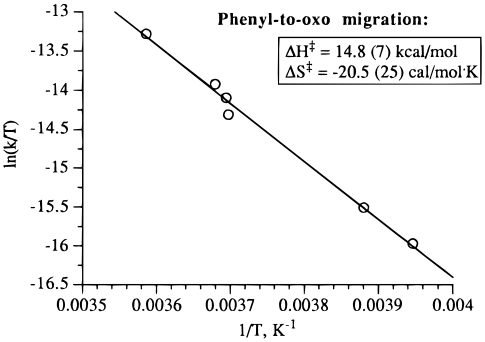

Figure 9. Eyring plot of phenyl oxidation in [(HBpz$_3$)ReO$_2$(Ph)]OTf in CD_2Cl_2.

(HBpz$_3$)ReO(OPh)(OTf), addition of pyridine or chloride forms the observed phenoxide products and reaction with pyridine *N*-oxide gives the catecholate. The yield of the catecholate complex from isolated (HBpz$_3$)ReO(OPh)(OTf) is only ∼30%, which is unexpected given the essentially quantitative recovery of oxidized products in the reactions of the dioxo−phenyl complex. A possible explanation is that the pyridine produced during the formation of [(HBpz$_3$)ReO$_2$(Ph)]OTf from (HBpz$_3$)-ReO(Ph)OTf plays a role in the oxidation of phenoxide to catecholate, as a proton must be removed in the process. Consistent with this proposal is the observation that when the oxidation of (HBpz$_3$)ReO(OPh)OTf is monitored at low temperature, the yield of catecholate is markedly higher in the later stages after pyridine has accumulated in solution. The catecholate complex reacts with pyridine *N*-oxide over the course of several days at room temperature to give a dark green solution containing uncharacterized rhenium products.

Since the slow step in forming the three observed oxidation products is phenyl-to-oxo migration, measuring the rate of formation of these products, taken together, measures the rate of phenyl migration. The reaction was monitored over time, and the appearance of the oxidation products was found to obey first-order kinetics (Figure 8) over 3 half-lives. The observed rate constant was not significantly altered by changing the concentrations of rhenium or pyridine *N*-oxide. This strongly suggests that the unobserved rhenium products are kinetically innocent. From rate measurements at temperatures from 253 to 279 K, activation parameters for the phenyl-to-oxo migration were found to be $\Delta H^{\ddagger} = 14.8(7)$ kcal/mol and $\Delta S^{\ddagger} = -20.5(25)$ eu (Figure 9).

The reaction of pyridine *N*-oxide with the rhenium phenyl triflate was run in the presence of molecular iodine to exclude the possible involvement of phenyl radicals. Though the modest enthalpy of activation and especially the negative $\Delta S^{\ddagger}$ are not consistent with a dissociative mechanism, the addition of iodine is a more definitive test because I_2 is an exquisitely fast trap

for phenyl radicals, reacting at essentially diffusion-limited rates (1.2×10^{10} M^{-1} s^{-1} in benzene[20]). Iodine reacts with $(HBpz_3)$-ReO(Ph)(OTf) at room temperature, but slowly enough that oxidation of the phenyl group may be carried out successfully: addition of excess pyridine *N*-oxide at room temperature gives the catecholate complex $(HBpz_3)ReO(O_2C_6H_4)$ as usual, excluding possible involvement of free phenyl radicals in the reaction.

Scope of Aryl Oxidation. Other aryl groups are also oxidized under analogous conditions. $(HBpz_3)ReO(2,4\text{-}Me_2C_6H_3)(OTf)$ is prepared by photolysis of $(HBpz_3)ReO(I)Cl$ in *m*-xylene,[10a] followed by treatment of the xylyl−chloride complex with silver triflate. This aryl triflate reacts with 1.6 equiv of C_5H_5NO in CD_2Cl_2 to produce, after treatment with Me_4NCl, a mixture of $(HBpz_3)ReO(O\text{-}2,4\text{-}Me_2C_6H_3)(Cl)$ and the 3,5-dimethylcatecholate complex $(HBpz_3)ReO(O_2C_6H_2Me_2)$ (eq 12). No other regioisomers are observed. This indicates

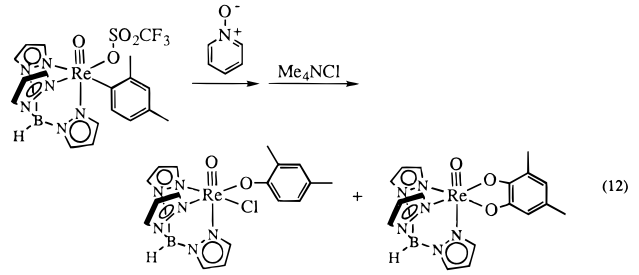

(12)

that the initial migration takes place at the *ipso* carbon and that oxidation to the catecholate takes place at an *ortho* position that has a hydrogen atom attached, i.e., without methyl group rearrangement.

Oxidation of the isomeric $(HBpz_3)ReO(3,4\text{-}Me_2C_6H_3)(OTf)$, obtained in a similar fashion, was examined with both pyridine *N*-oxide and dimethyl sulfoxide as oxidants. Oxidation with an excess of C_5H_5NO in CD_2Cl_2 at room temperature gave dimethylcatecholates as a 3.3:1 mixture of the symmetric (4,5-dimethyl) and asymmetric (3,4-dimethyl) isomers in 35% yield (eq 13).

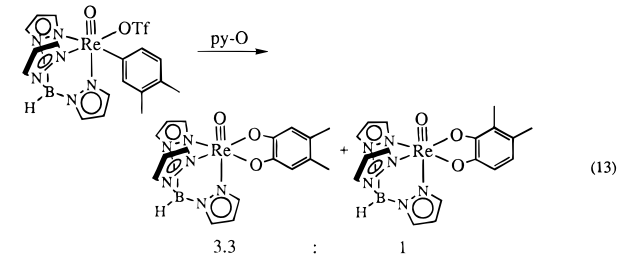

(13)

On reaction with Me_2SO, an adduct is formed (cf. eq 2) which rearranges to a single phenoxide product, $[(HBpz_3)ReO(OC_6H_3\text{-}Me_2)(OSMe_2)]OTf$, (eq 14) in ca. 80% yield based on converted

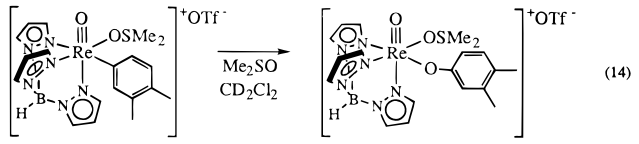

(14)

rhenium aryl complex. Again the substitution pattern of the starting material is preserved in the product. Me_2S dissociation from the adduct $[(HBpz_3)ReO(3,4\text{-}Me_2C_6H_3)(OSMe_2)]OTf$ occurs with a rate constant $k = 5.8(8)$ s^{-1} at 298 K, 2.0 times faster than observed for the phenyl complex.

To determine electronic effects on aryl oxidation, the oxidations of the 3,4-dimethylphenyl complex (eqs 13, 14) were monitored over time. Oxidation by pyridine *N*-oxide, for which the rate-limiting step is most likely aryl-to-oxo migration (see above), is >90% complete in 2 min at room temperature. The migration is therefore estimated to proceed at least 3 times more rapidly than oxidation of the phenyl complex, which has an extrapolated half-life of 4.2 min at 298 K. Oxidation by Me_2SO (eq 14) is also faster than the analogous oxidation of the phenyl complex, with the rate constant of $k = 4.3(3) \times 10^{-7}$ M s^{-1} being 6.3 times greater. The rate of oxidation of Me_2SO to Me_2SO_2 also increases, but by a factor of only 1.8 ($k = 4.6(11) \times 10^{-5}$ s^{-1} for the dimethylphenyl complex vs $k = 2.49(11) \times 10^{-5}$ s^{-1} for the phenyl complex). Aryl oxidation thus is accelerated by a factor of 3.5 relative to Me_2SO oxidation by $[(HBpz_3)ReO_2(Ar)]OTf$ on going from $Ar = C_6H_5$ to $Ar = 3,4\text{-}Me_2C_6H_3$. Any change in the equilibrium concentration of the intermediate would affect both of these oxidations equally. The observed difference in reactivity is therefore likely to be the result of a difference in migratory aptitude of the aryl groups, with the more electron-rich aryl group being more prone to migrate. A full study of substituent effects on the aryl migration is in progress.

Discussion

$[(HBpz_3)ReO_2(Ph)]OTf$ as an Electrophilic Oxidant. Highly oxidizing metal alkyl complexes are difficult to prepare because the conventional reagents used to alkylate transition metals, such as alkyllithium, alkylzinc, and Grignard reagents, are also good reducing agents. Ethylation of $(HBpz_3)ReOCl_2$ with Et_2Zn, for example, gives substantial amounts of reduced products,[10b] and alkyl- and aryllithium reagents give no alkylated products at all with this rhenium complex. Our route to rhenium(VII) oxo−alkyl[21] and −aryl complexes is the oxidation of a rhenium(V) precursor that already contains the metal−carbon bond. Thus, the rhenium(V) phenyl triflate complex $(HBpz_3)ReO(Ph)(OTf)$ reacts with oxygen atom donors to give the rhenium(VII) dioxo−phenyl complex $[(HBpz_3)ReO_2(Ph)]OTf$. Reaction with dimethyl sulfoxide gives the dioxo complex reversibly as a transient intermediate, while reaction with the more powerful oxidant pyridine *N*-oxide proceeds irreversibly to the dioxo−phenyl cation, which is stable at low temperature and may be observed directly by NMR. Though the broad lines in the NMR preclude definitive identification of the dioxo complex based on spectroscopic data alone, its identity is indicated on chemical grounds based on its rapid low-temperature reaction with Me_2S to form the rhenium(V) phenyl−dimethyl sulfoxide adduct.

The fluxionality of $[(HBpz_3)ReO_2(Ph)]OTf$ is unexpected, as the isoelectronic complex $[HB(3,5\text{-}Me_2pz)_3]WO_2(Ph)$ has a static NMR spectrum.[22] Facile dissociation of one arm of the tris(pyrazolyl)borate ligand is unlikely, as the rhenium(VII) complex $(Bpz_4)ReO_3$ does not show exchange between coordinated and free pyrazoles in the NMR.[23] A possible explanation for the difference between the neutral tungsten complex and the cationic rhenium analogue is that the triflate ligand may bind to the rhenium center to give a fluxional seven-coordinate compound. Triflate binds well to rhenium(V) (witness the short Re−O bonds in $[HBpz_3]ReO[OTf]_2$), and coordination to a cationic rhenium(VII) species, especially in a relatively nonpolar solvent like dichloromethane, is plausible. An equilibrium between a cationic six-coordinate structure and a neutral triflate

(20) Asmus, K.-D.; Bonifacic, M. In *Radical Reaction Rates in Liquids*; Fischer, H., Ed.; Landolt-Börnstein New Series; Springer-Verlag: Berlin, 1984; Vol. 13, Subvol. b, Carbon-Centered Radicals II, p 25.

(21) DuMez, D. D.; Mayer, J. M. *J. Am. Chem. Soc.*, in press.

(22) Eagle, A. A.; Young, C. G.; Tiekink, E. R. *Organometallics* **1992**, *11*, 2934−2938.

(23) Domingos, Â.; Marçalo, J.; Paulo, A.; de Matos, A. P.; Santos, I. *Inorg. Chem.* **1993**, *32*, 5114−5118.

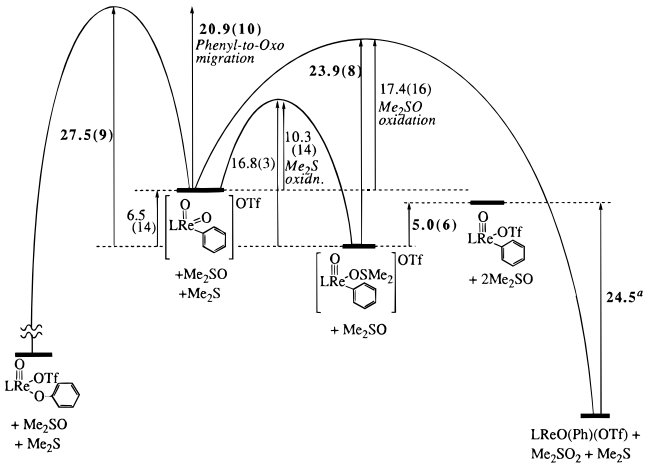

Figure 10. Potential energy surface for oxidations of $[(HBpz_3)ReO_2(Ph)]OTf$. All numbers are values of $\Delta G°$ at 298 K in kcal/mol. Values in boldface are directly measured quantities; those in normal type are calculated by difference. Estimated standard deviations in the last digit are in parentheses. L = $HBpz_3^-$. [a]Data from ref 25.

adduct would be consistent with the observed ^1H NMR spectra.[24] We have written the dioxo−phenyl complex in the cationic six-coordinate form $[(HBpz_3)ReO_2(Ph)]OTf$, though a neutral triflate complex could be the ground state. In any case, the fluxionality can be accounted for if the cationic and neutral forms are fairly close in energy.

The rates of phenyl-to-oxo migration have been measured directly from $[(HBpz_3)ReO_2(Ph)]OTf$ as generated irreversibly from pyridine *N*-oxide as well as indirectly from the Me_2SO adduct. The difference in rate in the two cases is the equilibrium constant for loss of Me_2S from $[(HBpz_3)ReO(Ph)(OSMe_2)]OTf$: $K_{diss} = 1.6 \times 10^{-5}$ M at 298 K. This places the dioxo complex and the sulfoxide adduct on a common energy scale. A detailed free energy diagram for the oxidation reactions of $[(HBpz_3)ReO_2(Ph)]OTf$ with both endogenous (the phenyl group) and exogenous (Me_2S, Me_2SO) substrates is shown in Figure 10; enthalpies and entropies of activation and reaction are listed in Scheme 3.[25] The only species that cannot be placed quantitatively on the diagram is the phenoxide complex $(HBpz_3)ReO(OPh)(OTf)$, though it must be at least 3 kcal/mol below the phenyl-sulfoxide complex based on its irreversible formation. $(HBpz_3)ReO(OPh)(OTf)$ is depicted in a position estimated by assuming that the Re−Ph → Re−OPh oxidation is energetically similar to H−Ph → H−OPh.[26]

The free energy diagram shows that $[(HBpz_3)ReO_2(Ph)]OTf$ oxidizes dimethyl sulfide with a very low barrier ($\Delta G^‡ = 10.2$ kcal/mol), corresponding to a rate of 1.7×10^5 M^{-1} s^{-1} at 298 K. It is very unlikely that this reaction occurs by electron transfer, given the difficulty of outer-sphere oxidation of dialkyl sulfides (E_p for Me_2S oxidation in CH_3CN is 1.71 V vs SCE[27]). The measured barrier requires that the dioxo−phenyl have a redox potential of at least 1.27 V. The related dioxo-chloride complex, which should be significantly more oxidizing than the

Scheme 3. Enthalpies (kcal/mol) and Entropies (cal/mol K) of Activation and of Reaction for Reactions of $[(HBpz_3)ReO_2(Ph)]OTf$ and Related Species in CD_2Cl_2

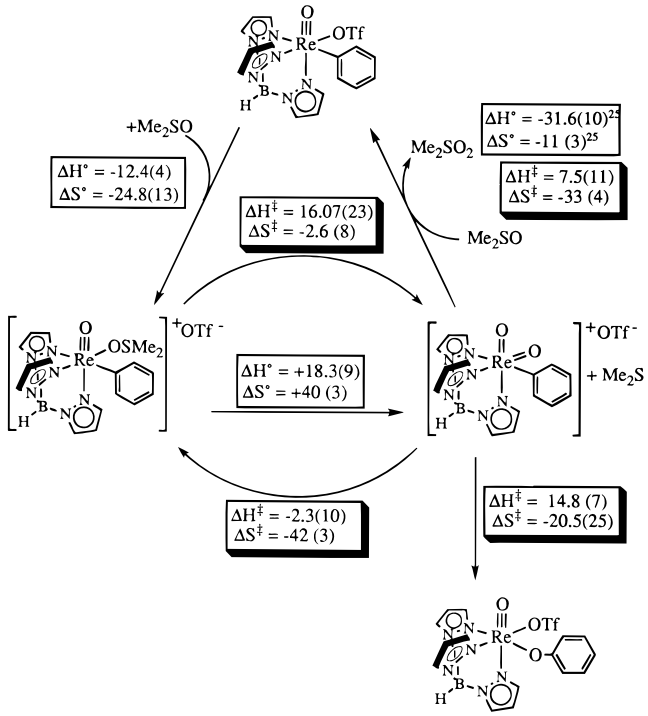

phenyl analogue, exhibits an $E_{1/2}$ of 1.33 V (in CH_3CN, vs SCE).[28] Thus Me_2S oxidation almost undoubtedly occurs by attack of sulfur at an oxo group, by oxygen atom transfer. The speed of the oxidation is remarkable compared with other transition metal oxo species. For instance, the reactive ruthenium(IV) oxo complex $[(bpy)_2(py)RuO]^{2+}$ studied by Meyer and co-workers reacts with Me_2S at a rate of only 17.1 M^{-1} s^{-1}.[29] Other ruthenium(IV)[30] and ruthenium(VI)[31] oxo complexes that have been studied react at similar or slower rates. The 10^4 rate difference between rhenium and ruthenium occurs in spite of the fact that the rhenium(VII) complex is a weaker oxidant than ruthenium(IV), as can be seen from a comparison of eqs 15 and 16.[32] Analogously, Me_2S loss from $[(HBpz_3)$-

$$[(HBpz_3)ReO_2(Ph)]OTf + Me_2S \rightarrow [(HBpz_3)ReO(Ph)(OSMe_2)]OTf \quad (15)$$

$$\Delta G° = -6.4 \text{ kcal/mol}$$

$$[(bpy)_2(py)Ru(O)]^{2+}(aq) + Me_2S(g) + H_2O(aq) \rightarrow [(bpy)_2(py)Ru(OH_2)]^{2+}(aq) + Me_2SO(g) \quad (16)$$

$$\Delta G° = -17.9 \text{ kcal/mol}$$

(24) The triflate adduct could be seven-coordinate or six-coordinate, with triflate displacing one arm of the $HBpz_3$ ligand. For other examples of hapticity changes in (pyrazolylborate)rhenium complexes, see: Paulo, A.; Domingos, Â; Santos, I. *Inorg. Chem.* **1996**, *35*, 1798−1807.

(25) Thermodynamic data on gas-phase Me_2S, Me_2SO, and Me_2SO_2 are from Wagman, D. D.; Evans, W. H.; Parker, V. B.; Schumm, R. H.; Halow, I.; Bailey, S. M.; Churney, K. L.; Nuttall, R. L. *J. Phys. Chem. Ref. Data* **1982**, *11*, Suppl. no. 2. Indicated values for the oxidation of Me_2SO neglect any differential solvation of $2Me_2SO$ vs $Me_2S + Me_2SO_2$.

(26) Gas-phase ΔG values are taken from Barin, I. *Thermochemical Data of Pure Substances, Part I*; VCH: Weinheim, Germany, 1989.

(27) Cottrell, P. T.; Mann, C. K. *J. Electrochem. Soc.* **1969**, *116*, 1499−1503.

(28) DuMez, D. D.; Mayer, J. M. Unpublished results. $E_{1/2}$ measured vs $Cp_2Fe^{+/0}$ and converted to SCE according to Connelly, N. G.; Geiger, W. E. *Chem. Rev.* **1996**, *96*, 877−910.

(29) Roecker, L.; Dobson, J. C.; Vining, W. J.; Meyer, T. J. *Inorg. Chem.* **1987**, *26*, 779−781.

(30) Acquaye, J. H.; Muller, J. G.; Takeuchi, K. J. *Inorg. Chem.* **1993**, *32*, 160−165.

(31) Rajapakse, N.; James, B. R.; Dolphin, D. *Stud. Surf. Sci. Catal.* **1990**, *55*, 109−117.

(32) Reduction potentials vs NHE for $[(bpy)_2(py)Ru(O)]^{2+}(aq) + 2e^- + 2H^+ \rightarrow [(bpy)_2(py)Ru(OH_2)]^{2+}(aq)$ from Moyer, B. A.; Meyer, T. J. *Inorg. Chem.* **1981**, *20*, 436−444. $E° = 1.229$ V for $^1/_2$ $O_2(g) + 2$ $e^- + 2H^+ \rightarrow H_2O(l)$ from Hoare, J. P. In *Encyclopedia of Electrochemistry of the Elements*; Bard, A. J., ed.; M. Dekker: New York, 1974; Vol II; Chapter II-5, p 193. Together these give the free energy for $[(bpy)_2(py)Ru(O)]^{2+}(aq) + H_2O$ (l) → $[(bpy)_2(py)Ru(OH_2)]^{2+}(aq) + ^1/_2$ O_2 (g). Addition of the $\Delta G°$ values for $Me_2S(g)$ and $Me_2SO(g)$[25] gives eq 16.

$ReO(Ph)(OSMe_2)]OTf$ is almost 2000 times faster than from $MoO(LNS_2)(OSMe_2)$ (LNS_2 = 2,6-bis(2,2-diphenyl-2-mercaptoethyl)pyridine),[33] even though sulfide extrusion must be at least 9 kcal/mol less favorable for rhenium than for molybdenum since Mo(IV) is completely oxidized to Mo(VI) by Me_2SO.

Insight into the high kinetic reactivity of $[(HBpz_3)ReO_2(Ph)]$-OTf can be gained by examining its relative reactivity with Me_2S and Me_2SO. The kinetic preference of oxidants for sulfide vs sulfoxide oxidation has been used as a gauge of the electrophilicity or nucleophilicity of an oxidant.[34,35] Nucleophilic oxidants such as HO_2^- react with sulfoxides more rapidly than with sulfides, while electrophilic oxidants show the reverse selectivity. For example, one study found that peroxides in acidic solution, among the most electrophilic reagents studied, reacted with sulfides up to 140 times more readily than with sulfoxides.[34] While $[(HBpz_3)ReO_2(Ph)]OTf$ does react rapidly with Me_2SO (k = 1.6 M^{-1} s^{-1} at 298 K), it is an incredible $1.2(2) \times 10^5$ times more reactive toward Me_2S. Quantitative comparison of this value with those observed for organic oxidants is complicated by the possibility of differential binding to the metal center—Me_2SO forms a stable adduct with $[HBpz_3]ReO(Ph)(OTf)$ while Me_2SO_2 does not—which may somewhat exaggerate the preference toward sulfide oxidation. However, $[(bpy)_2(py)Ru{=}O]^{2+}$, which shows the same pattern of ligand binding, exhibits a k_{Me_2S}/k_{Me_2SO} of only 128.[29] Other metal oxo complexes show comparable[30] or substantially lower[36] selectivities.[37] The 10^5 selectivity of $[(HBpz_3)ReO_2(Ph)]OTf$ therefore establishes it, according to this criterion, as an exceptionally electrophilic oxidant.

The enthalpic barrier for Me_2S oxidation, derived from the $\Delta H^{\ddagger}$ values for the two phenyl migrations and Me_2S dissociation (Scheme 3), is negative ($\Delta H^{\ddagger} = -2.3(10)$ kcal/mol), though the relatively large error bars indicate that the value is within experimental error of zero.[38] Such a small barrier is consistent with $[(HBpz_3)ReO_2(Ph)]OTf$ acting as an electrophile. This is of interest since few oxo complexes, and no oxo—alkyl complexes, have heretofore been established as strong electrophiles.[39] One factor that may contribute to the electrophilicity of this dioxo complex is its positive charge. For example, of the rhenium(V) oxo complexes $(HBpz_3)ReOCl_2$ and $[(tacn)ReOCl_2]^+$ (tacn = 1,4,7-triazacyclononane), the latter cationic complex reacts much more readily with triphenylphosphine, being deoxygenated within a day at room temperature,[40] while the neutral tris(pyrazolyl)borate complex requires heating overnight to be deoxygenated.[10b,11b] Cationic chromium(V) oxo complexes with substituted salen ligands have also been characterized as electrophilic and are reported to oxidize relatively nucleophilic substrates (e.g., norbornene) in the presence of dimethyl sulfoxide as an inert coligand.[41] Another factor enhancing the electrophilicity of $[(HBpz_3)ReO_2(Ph)]OTf$ is its high oxidation state. However, since the cationic *trio*xo complexes $[(tacn)ReO_3]^+$ and $[(Me_3tacn)ReO_3]^+$ are only mildly electrophilic,[40] the fact that $[(HBpz_3)ReO_2(Ph)]OTf$ is a dioxo complex must also be significant. Addition to the oxo ligand results in formal reduction of the metal, and *cis*-oxo ligands are expected to have unfavorable interactions with the two d electrons in the reduced species. Thus, while few *cis*-dioxo complexes of rhenium(V) are known,[42] monooxorhenium(V) complexes such as would be formed by nucleophilic attack at an oxo ligand of $[(HBpz_3)ReO_2(Ph)]OTf$ are abundant and generally robust.

Metal-to-Oxo Migrations of σ-Bonded Organometallic Groups. The rhenium(VII) dioxo complex $[(HBpz_3)ReO_2(Ph)]$-OTf undergoes facile metal-to-oxo migration of its phenyl ligand to form phenoxide. The migration is first order in the dioxo complex, and its rate is unaffected by the presence of additional oxidants such as pyridine *N*-oxide or DMSO. It does not involve metal—carbon bond homolysis since it proceeds with a substantial negative entropy of activation and is unaffected by the presence of I_2. Finally, reactions with substituted aryl groups produce only the products of *ipso* attack. In short, the migration is a simple [1,2]-phenyl shift.

Metal-to-oxo migrations in metal oxo—alkyl and —aryl complexes are rare. This is the first case in which a thermal reaction has been well-established, though there are a handful of cases in the literature where metal-to-oxo,[3] -imido,[5] or -sulfido[6] migrations have been invoked in thermal reactions on the basis of indirect evidence. In view of the large and growing number of stable oxo—alkyl complexes that have been synthesized, the general absence of this mode of reactivity suggests that it is simply not a facile transformation. In some cases the absence of this reaction is likely due to greater thermodynamic stability of the oxo—alkyls over their alkoxide isomers, but a number of remarkably high oxidation state oxo—alkyls have been synthesized in recent years for which the transformation of eq 1 appears thermodynamically accessible. Examples include $V(O)R_3$,[4b,6] $Cp^*CrO_2(CH_3)$ and $Cp^*CrO(CH_3)_2$,[43] (HB[3,5-

(33) Berg, J. M.; Holm, R. H. *J. Am. Chem. Soc.* **1985**, *107*, 925—932.

(34) Adam, W.; Haas, W.; Lohray, B. B. *J. Am. Chem. Soc.* **1991**, *113*, 6202—6208 and references therein.

(35) While the substrate typically used in this assay, thianthrene 5-oxide, is convenient in that it contains both a sulfoxide and a sulfide in the same molecule, simpler sulfides and sulfoxides are suitable probes as well. In some cases monofunctional substrates have been reported to be preferable since they avoid the electron-transfer side reactions that can intervene with the heterocyclic thianthrene oxide. See, e.g.: Ballisteri, F. P.; Tomaselli, G. A.; Toscano, R. M.; Conte, V.; DiFurio, F. *J. Am. Chem. Soc.* **1991**, *113*, 6209—6212.

(36) (a) (Porphyrin)RuO_2 complexes: ref 31. Higuchi, T.; Ohtake, H.; Hirobe, M. *Tetrahedron Lett.* **1991**, *32*, 7435—7438. (b) RuO_4: Djerassi, C.; Engle, R. R. *J. Am. Chem. Soc.* **1953**, *75*, 3838—3841. (c) $NaMnO_4$, OsO_4: Henbest, H. B.; Khan, S. A. *Chem. Commun.* **1968**, 1036.

(37) Thioether oxidations by hydrated $H_5PV_2Mo_{10}O_{40}$ are highly selective to the sulfoxide, although interpretation is complicated by protonation of the sulfoxides under some of the reaction conditions and by the possibility of an electron-transfer mechanism. Gall, R. D.; Faraj, M.; Hill, C. L. *Inorg. Chem.* **1994**, *33*, 5015—5021.

(38) (a) Negative activation enthalpies are unusual but precedented. Negative $\Delta H^{\ddagger}$ values can arise from a rapid exothermic preequilibrium followed by a rate-limiting step with a positive $\Delta H^{\ddagger}$, so that the sum of the enthalpies of the two steps is negative.[38b] The preequilibrium in this case could involve triflate binding in the $[(HBpz_3)ReO_2(Ph)]OTf$ intermediate. Negative $\Delta H^{\ddagger}$ values have also been observed in highly exothermic bimolecular reactions, such as radical recombination reactions[38c] and certain electron-transfer reactions.[38d] (b) See, e.g.: Jähme, J.; Rüchardt, C. *Tetrahedron Lett.* **1982**, 4011—4014. Albrecht-Gary, A.-M.; Dietrich-Buchecker, C.; Saad, Z.; Sauvage, J.-P. *J. Chem. Soc., Chem. Commun.* **1992**, 280—282. Rexwinkel, R. B.; Meskers, S. C. J.; Riehl, J. P.; Dekkers, H. P. J. M. *J. Phys. Chem.* **1993**, *97*, 3875—3884. Kirowa-Eisner, E.; Schwarz, M.; Rosenblum, M.; Gileadi, E. *J. Electrochem. Soc.* **1994**, *141*, 1183—1190. (c) Olson, J. B.; Koch, T. H. *J. Am. Chem. Soc.* **1986**, *108*, 756—761. Kerr, J. A., Ed. *Handbook of Bimolecular and Termolecular Gas Reactions*; CRC Press: Boca Raton, FL, 1981; Vol. II. (d) Patel, R. C.; Ball, R. E.; Endicott, J. F.; Hughes, R. G. *Inorg. Chem.* **1970**, *9*, 23—27. Meyer, T. J.; Braddock, J. N. *J. Am. Chem. Soc.* **1973**, *95*, 3158—3162.

(39) For examples of electrophilic reactivity of terminal imido complexes, see: (a) Luan, L.; Brookhart, M.; Templeton, J. L. *Organometallics* **1992**, *11*, 1433 and references therein. (b) Coia, G. M.; White, P. S.; Meyer, T. J.; Wink, D. A.; Keefer, L. K.; Davis, W. M. *J. Am. Chem. Soc.* **1994**, *116*, 3649—3650 and references therein. (c) Mahy, J.-P.; Bedi, G.; Battioni, P.; Mansuy, D. *J. Chem. Soc., Perkin Trans. 2* **1988**, 1517—1524. (d) Wigley, D. E. *Prog. Inorg. Chem.* **1994**, *42*, 239—482, especially pp 264—266.

(40) Conry, R. R.; Mayer, J. M. *Inorg. Chem.* **1990**, *29*, 4862—4867. Wieghardt, K.; Pomp, C.; Nuber, B.; Weiss, J. *Inorg Chem.* **1986**, *25*, 1659—1661. Pomp, C.; Wieghardt, K. *Polyhedron* **1988**, *7*, 2537—2542.

(41) Samsel, E. G.; Srinivasan, K.; Kochi, J. K. *J. Am. Chem. Soc.* **1985**, *107*, 7606—7617.

(42) Blackburn, R. L; Jones, J. M.; Ram, M. S.; Sabat, M.; Hupp, J. T. *Inorg. Chem.* **1990**, *29*, 1791—1792. Ram, M. S.; Hupp, J. T. *Inorg. Chem.* **1991**, *30*, 130—133. Ciani, G. F.; D'Alfonso, G.; Romiti, P. F.; Sironi, A.; Freni, M. *Inorg. Chim. Acta* **1983**, *72*, 29—37.

(43) Noh, S.-K.; Heintz, R. A.; Haggerty, B. S.; Rheingold, A. L.; Theopold, K. H. *J. Am. Chem. Soc.* **1992**, *114*, 1892—1893.

$Me_2pz]_3)MoO_2(R)$,[44] $CpMoO_2(R)$[45] and related oxo−sulfido complexes,[46] $(HB[3,5\text{-}Me_2pz]_3)WO_2(R)$,[22] $ReO_2(CH_2SiMe_3)_3$,[47] $CH_3Re(O)_2(O_2C_6H_4)(py)$,[48] and $OsO_2(mesityl)_2$.[49] The reverse reaction, transformation of an alkoxide into an oxo−alkyl, is also extremely rare. Of the welter of known alkoxide complexes, only one example has been observed to undergo oxygen-to-metal migration.[8] In the few cases where oxo−alkyl and corresponding alkoxide complexes have both been studied—$(RC{\equiv}CR)_2ReO(R')$ and $(RC{\equiv}CR)_3Re(OR')$,[12] $(HBpz_3)ReO(R)Cl$ and $(HBpz_3)Re(OR)(Cl)(L)$,[10] and $[Cp^*_2Ta(OCH_3)]$ and $Cp^*_2Ta(O)CH_3$[8]—a substantial kinetic barrier to interconversion has been found. In the first two cases no thermal migrations of alkyl groups are observed, while the last requires high temperatures.

We propose that the electrophilicity of the oxo groups in $[(HBpz_3)ReO_2(Ph)]OTf$ is the key feature that allows facile phenyl migration from metal to oxygen. The importance of electrophilicity in organic [1,2]-shifts, from carbocation rearrangements to Baeyer−Villiger oxidations, is well-established.[50] In these [1,2]-migrations, the electrons in the σ bond that is broken interact favorably with an empty orbital at the migration terminus, maintaining bonding throughout. Alkyl and hydride shifts are ubiquitous in carbocation chemistry and often proceed with extremely small kinetic barriers.[51] In carbanions, the orbital at the migration terminus is filled and creates an antibonding interaction in the transition state. Alkyl groups therefore do not migrate in simple carbanions.

A good analogy may be drawn between carbocation rearrangements and the most common example of [1,2]-shift in organometallic chemistry, migrations to carbonyl ligands.[52,53] The two reactions are analogous electronically in that the migrating group is formally an anion, neutralizing the carbocationic site or turning the neutral carbonyl into an anionic acyl ligand. This similarity appears to have some reality beyond the formal level as well: Increasing the electrophilicity of a carbonyl increases its reactivity toward migratory insertion,[54] and electron-rich alkyls have greater migratory aptitude,[52b] as is also seen in organic systems.[55] Finally, in all cases that have been studied, carbonyl insertions proceed with retention of configuration at the migrating alkyl group,[52] as is observed in carbocation rearrangements.

Just as metal-to-carbonyl migrations parallel carbocation rearrangements, so too do metal-to-oxo rearrangements appear to parallel carbanion rearrangements. In both of the latter reactions the migrating group moves as a cation: The dinegative oxo ligand becomes a uninegative alkoxide. Furthermore, the reactivity in the two cases is very similar—usually, there is none. Apart from this negative evidence, an examination of the exceptional cases in both reaction classes reveals similarities. There are two main classes of carbanion-type [1,2]-shifts that do take place in organic chemistry. First, while alkyl groups do not migrate in carbanions, aryl groups can, due to the availability of π^* orbitals on the benzene ring.[50] In this light it is perhaps suggestive that the cases in which metal-to-oxo (or -imido, or -sulfido) migration has been proposed have all involved the migration of aryl rather than alkyl groups.[3,5,6] In particular, Nugent and co-workers[5] found that while methylation with dimethylzinc of a *tert*-butylimido complex led to an isolable organometallic product, analogous treatment with diphenylzinc led to *N*-*tert*-butylaniline (after workup), attributed to phenyl-to-nitrogen migration. The second, more abundant class of observed organic electrophilic rearrangements is typified by the Stevens (e.g., eq 17)[56,57] and Wittig (e.g., eq 18)[56] rearrangements. These and related reactions involve highly favorable

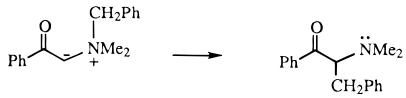

(17)

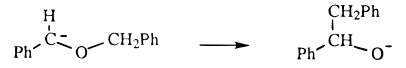

(18)

transfers of alkyl groups driven by concomitant transfer of negative charge from carbon to a more electronegative atom. These reactions are generally accepted to proceed by carbon−heteroatom bond homolysis, with variable amounts of geminate and intermolecular recombination. Thus, the observed stereochemistry ranges from complete retention of configuration to complete racemization.[58,59] In metal systems, the partial (ca. 15%) loss of stereochemistry observed by Bercaw and co-workers in the migration of a deuterated phenethyl group from sulfur to tantalum[60] is reminiscent of the stereochemical results of Stevens rearrangements.[58] This result suggests the possibility of a homolytic mechanism (though the possibility of loss of stereochemistry in an earlier step could not be excluded). Recent studies on the deoxygenation of alcohols by tungsten(II) phosphine complexes show that alkyl radicals are intermediates in at least some cases,[61] in contrast to earlier suggestions.[62] Presumably carbon−oxygen bond homolysis is the origin of these radicals. Also noteworthy is the much higher migratory aptitude of hydrogen as compared to alkyl in $[Cp^*_2Ta(OR)]$[8] and $(RC{\equiv}CR)_3Re(OR')$.[9,12] Electrophilic migration of hydrogen is just proton transfer and has a huge advantage over alkyl migration, while hydride migration is at best only mildly favored over alkyl migration in carbocationic (nucleophilic) shifts.[63]

The one instance in which the organic analogy fails for metal-to-oxo migrations is, of course, the phenyl-to-oxo migration of $[(HBpz_3)ReO_2(Ph)]OTf$ described in this report. In the cationic dioxo complex, migration is thermally facile, with an extrapolated half-life of roughly 4 min at room temperature. Further-

(44) Onishi, M.; Ikemoto, K.; Hiraki, K.; Koga, R. *Bull. Chem. Soc. Jpn.* **1993**, *66*, 1849−1851.
(45) Legzdins, P.; Phillips, E. C.; Sánchez, L. *Organometallics* **1989**, *8*, 940−949.
(46) Faller, J. W.; Ma, Y. *Organometallics* **1989**, *8*, 609−612.
(47) Cai, S.; Hoffman, D. M.; Wierda, D. A. *Organometallics* **1988**, *7*, 2069−2070.
(48) Takacs, J.; Kiprof, P.; Riede, J.; Herrmann, W. A. *Organometallics* **1990**, *9*, 782−787.
(49) Stavropoulos, P.; Edwards, P. G.; Behling, T.; Wilkinson, G.; Motevalli, M.; Hursthouse, M. B. *J. Chem. Soc., Dalton Trans.* **1987**, 169.
(50) Harwood, L. M. *Polar Rearrangements*; Oxford University Press: New York, 1992; p 60.
(51) Ahlberg, P.; Jonsäll, G.; Engdahl, C. *Adv. Phys. Org. Chem.* **1983**, *19*, 223−379.
(52) (a) Wojcicki, A. *Adv. Organomet. Chem.* **1973**, *11*, 87. (b) Kuhlman, E. J.; Alexander, J. *Coord. Chem. Rev.* **1980**, *33*, 195.
(53) Berke, H.; Hoffmann, R. *J. Am. Chem. Soc.* **1978**, *100*, 7224.
(54) Richmond, T. G.; Basolo, F.; Shriver, D. F. *Inorg. Chem.* **1982**, *21*, 1272−1273 and references therein.
(55) March, J. *Advanced Organic Chemistry*, 4th ed.; John Wiley and Sons: New York, 1992; pp 1058−1061.
(56) Stevens, T. S. *Prog. Org. Chem.* **1968**, *7*, 48−74. Zimmermann, H. E. In *Molecular Rearrangements*; de Mayo, P., Ed. New York, Interscience Publishers: New York, 1963; Vol. I, pp 345−506.
(57) Pine, S. H. *Org. React.* **1970**, *18*, 403−464.
(58) Ollis, W. D.; Rey, M.; Sutherland, I. O. *J. Chem. Soc., Chem. Commun.* **1975**, 573. Dolling, U. H.; Closs, G. L.; Cohen, A. H.; Ollis, W. D. *J. Chem. Soc., Chem. Commun.* **1975**, 545.
(59) For a recent example of the stereochemical complexity of the Stevens rearrangement, see: Stará, I. G.; Starý, I.; Tichý, M.; Závada, J.; Hanuš, V. *J. Am. Chem. Soc.* **1994**, *116*, 5084−5088.
(60) Nelson, J. E.; Parkin, G.; Bercaw, J. E. *Organometallics* **1992**, *11*, 2181−2189.
(61) Crevier, T. J.; Mayer, J. M., Unpublished results.
(62) Jang, S.; Atagi, L. M.; Mayer, J. M. *J. Am. Chem. Soc.* **1990**, *112*, 6413−6414.
(63) Shubin, V. G. *Top. Curr. Chem.* **1984**, *117*, 267−341.

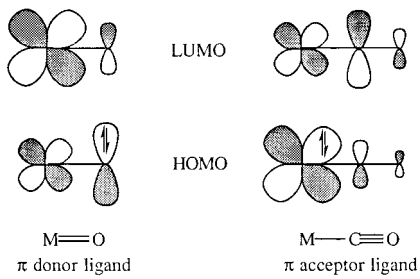

Figure 11. Comparison of bonding in typical metal oxo and metal carbonyl complexes.

more, the electron-donating substituents in the 3,4-dimethylphenyl complex appear to accelerate the migration, suggesting that the aryl group is donating rather than accepting electron density during the migration. The oxo ligand therefore acts as an electrophile in its oxidation of the coordinated phenyl group, just as it does in its oxidation of external reductants such as Me_2S. In summary, for this oxo complex, the [1,2]-migration of the aryl group appears to be similar not to a carbanion shift, but to migrations to a carbocation center or a carbonyl ligand.

An oxo group can act like a carbonyl because the factors that determine the electrophilic vs nucleophilic character of these ligands are more subtle than those that operate in the organic species. A carbocation has an empty orbital and a carbanion a filled one at the site which serves as the migration terminus. Metal carbonyls and metal oxo complexes do not differ in orbital occupancy (Figure 11). The distinction in their electrophilicities has to do with the character of the LUMO in the metal complexes, the site of electrophilic attack. The LUMO is low-lying and predominantly carbon-based in carbonyl compounds, enabling migration to this center. In metal oxo species the LUMO is metal-based and the oxo ligand is typically nucleophilic. However, the carbonyl/oxo distinction is merely qualitative in these essentially isoelectronic species, so one anticipates a continuum of reactivity rather than the stark dichotomy observed for R^+ vs R^-.

Migrations in oxo complexes are expected to become more facile the more the metal oxo bonding resembles that of metal carbonyls, that is, as the metal oxo π^* orbital drops in energy and acquires more oxygen character. This is what it means for an oxo complex to be electrophilic at oxygen. In this light, it is not surprising that the highly electrophilic $[(HBpz_3)ReO_2(Ph)]OTf$ is uniquely capable of undergoing phenyl-to-oxo migration. The analogy between this migration and migrations to carbonyl ligands is supported by the similar modest accelerations on 3,4-dimethyl substitution of the phenyl group in both cases.[64] The chemistry of the oxo groups in $[(HBpz_3)ReO_2(Ph)]OTf$ may be plausibly compared with that of π-acid ligands, for instance the electrophilic cationic carbene $[CpFe(CO)_2CH_2]^+$.[65] Loss of Me_2S from $[(HBpz_3)ReO(Ph)(OSMe_2)]^+$ is directly analogous to the loss of thioether from the protected carbene $[CpFe(CO)_2CH_2SR_2]^+$ (R = Me, Ph).[66,67]

This model has important consequences for future work. Attempts to design systems which oxidize hydrocarbons using metal-to-oxo migration should concentrate on species such as cations that are expected to have enhanced electrophilicity. Furthermore, alkyl groups as well as aryl groups should be able to migrate, as they do in rearrangements to carbocations. This is important, since alkyl, rather than aryl, migration is of more general interest in terms of both alkane and alkene oxidations. The migration observed in the present study may be assisted by the π system of the migrating aryl group; a more extensive study of substituent effects, now underway, may clarify the extent of assistance.

Scheme 4. Skeleton Mechanism for Osmylation of Olefins Proposed by Sharpless *et al.*[2]

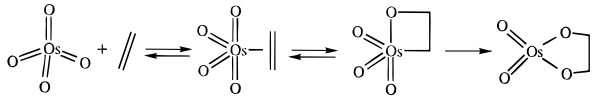

It is perhaps appropriate, in light of this new perspective on metal-to-oxo migrations, to comment on the most famous invocation of the reaction, that proposed by Sharpless two decades ago in his suggested mechanism for the osmylation of olefins (Scheme 4).[2] This mechanistic proposal continues to inspire lively debate,[2,68] but attention has focused almost exclusively on the formation of the metallaoxetane intermediate.[69] The subsequent step, ring expansion by metal-to-oxo migration (eq 1), merits at least as much attention, in view of the scanty precedent.[70]

The present work shows that facile metal-to-oxo migration is indeed possible, but only if the oxo ligand is sufficiently electrophilic. Given the difficulty of assessing the electrophilicity of the putative alkylosmium(VIII) trioxo complex without such a compound in hand, this conclusion cannot be applied directly to the Sharpless osmylation mechanism. It is ironic, however, that this perspective is exactly opposite to the original rationale for proposing organometallic intermediates. Sharpless and co-workers suggested the intermediacy of metal-bound intermediates to obviate the necessity for nucleophilic attack by an olefin on a metal oxo linkage polarized M^+-O^-.[2a] The analysis of the migration reaction presented in this study indicates that if the metal oxo linkage really is polarized in this fashion to give a nucleophilic oxo center, then alkyl migration will be kinetically unfavorable. If Sharpless' multistep mechanism does in fact operate, it does so for reasons quite different from those originally enunciated.

Conclusions

The rhenium(VII) dioxo−phenyl complex $[(HBpz_3)ReO_2(Ph)]OTf$ is formed on oxygen atom transfer to $(HBpz_3)ReO(Ph)OTf$. Using pyridine *N*-oxide, the dioxo−phenyl complex is observed at low temperatures. With Me_2SO, the adduct $[(HBpz_3)ReO(Ph)(Me_2SO)]OTf$ is stable at ambient temperatures, although it is in very rapid equilibrium with the dioxo complex via Me_2S loss. In both cases, the phenyl ligand migrates to an oxo group to give a phenoxide complex. The half-life for $[(HBpz_3)ReO_2(Ph)]OTf \rightarrow [(HBpz_3)ReO(OPh)L]OTf$ rearrangement is 4 min at 25 °C. This is the first clear example of thermal migration of a ligand from a metal center

(64) Garrou, P. E.; Heck, R. F. *J. Am. Chem. Soc.* **1976**, *98*, 4115−4127. Sugita, N.; Minkiewicz, J. V.; Heck, R. F. *Inorg. Chem.* **1978**, *17*, 2809−2813. Cross, R. J.; Gemmill, J. *J. Chem. Soc., Dalton Trans.* **1981**, 2317−2320

(65) Sanders, A.; Cohen, L.; Giering, W. P.; Kenedy, D.; Magatti, C. V. *J. Am. Chem. Soc.* **1973**, *95*, 5430.

(66) Brookhart, M.; Studabaker, W. B. *Chem. Rev.* **1987**, *87*, 411−432 and refs. therein.

(67) (a) Brandt, S.; Helquist, P. *J. Am. Chem. Soc.* **1979**, *101*, 6473−6475. (b) Barefield, E. K.; McCarten, P.; Hillhouse, M. C. *Organometallics* **1985**, *4*, 1682−1684.

(68) Corey, E. J.; Noe, M. C. *J. Am. Chem. Soc.* **1993**, *115*, 12579−12580. Kolb, H. C.; Andersson, P. G.; Bennani, Y. L.; Crispino, G. A.; Jeong, K.-S.; Kwong, H.-L.; Sharpless, K. B. *J. Am. Chem. Soc.* **1993**, *115*, 12226−12227. Norrby, P.-O.; Kolb, H. C.; Sharpless, K. B. *Organometallics* **1994**, *13*, 344−347. Gable, K. P.; Juliette, J. J. J. *J. Am. Chem. Soc.* **1995**, *117*, 955−962.

(69) (a) de With, J.; Horton, A. D.; Orpen, A. G. *Organometallics* **1993**, *12*, 1493−1496. (b) Walsh, P. J.; Hollander, F. J.; Bergman, R. G. *Organometallics* **1993**, *12*, 3705−3723. (c) Bennett, J. L.; Wolczanski, P. T. *J. Am. Chem. Soc.* **1994**, *116*, 2179−2180.

(70) Some discussion of this step can be found in Gable, K. P.; Juliette, J. J. J. *J. Am. Chem. Soc.* **1996**, *118*, 2625−2633.

to an oxo ligand. Kinetic and mechanistic studies indicate that this is a unimolecular rearrangement and provide a detailed view of the potential energy surface (Figure 10). The oxo ligands in [(HBpz$_3$)ReO$_2$(Ph)]OTf are suggested to be highly electrophilic, based on the very rapid reaction of the complex with Me_2S (10^5 M^{-1} s^{-1}), which is much faster than its oxidation of Me_2SO. The presence of a highly electrophilic oxo group is suggested to be the key feature in enabling metal-to-oxo migration. There are strong analogies between this migration and migrations to carbonyl ligands in organometallic compounds and electrophilic rearrangements in organic chemistry.

Experimental Section

General Considerations. ^{1}H and ^{13}C{^{1}H} NMR spectra were acquired on a Bruker AF-300 spectrometer at 300 and 75.4 MHz, respectively. ^{19}F NMR spectra were obtained on a Bruker AC-200 spectrometer at 188.298 MHz and were referenced to external CF_3-COOH at 0 ppm. Temperatures were measured using a thermocouple calibrated using the peak separation in neat CH_3OH.[71] All NMR spectra were obtained in dichloromethane-d_2 (CD_2Cl_2) unless otherwise noted. Peaks in the ^{1}H NMR due to the pyrazoles are listed by multiplicity only, 4-Hs as triplets and 3- and 5-Hs as doublets; all coupling constants are 2 Hz. CD_2Cl_2 was dried over CaH_2 and stored in a greaseless glass vessel with a Teflon needle valve. IR spectra were obtained on a Perkin-Elmer 1604 FT-IR spectrometer; peaks are reported in wavenumbers, and the relatively invariant bands associated with the HBpz$_3$ ligand[11a] are not listed. Electron impact mass spectra were acquired on a Kratos Analytical mass spectrometer in the positive ion mode, with samples introduced as solids in the direct inlet probe. Fast atom bombardment mass spectra (FABMS) were obtained using a VG 70 SEQ tandem hybrid instrument of EBqQ geometry, equipped with a standard saddle-field gun (Ion Tech Ltd., Middlesex, U.K.) producing a beam of xenon atoms at 8 keV and 1 mA. Samples were applied to the FAB target as solutions in dichloromethane. Matrices used included 3-nitrobenzyl alcohol and 2-hydroxyethyl disulfide. All spectra were taken in the positive ion mode. Elemental analyses were performed by Canadian Microanalytical Services, Ltd., Vancouver, BC.

Silver trifluoromethanesulfonate (silver triflate, AgOTf) and trimethylsilyl triflate were purchased from Aldrich and stored in the glovebox, at −20 °C and room temperature, respectively. Dimethyl sulfide (Aldrich) was dried over sodium, stored in a glass vessel with a Teflon needle valve, and vacuum transferred as needed. Pyridine *N*-oxide (py-O) was sublimed before use and stored in the drybox. ^{18}O-enriched dimethyl sulfoxide was synthesized according to a literature procedure;[72] the enrichment was found to be 50% by GC−MS. (HBpz$_3$)ReOCl$_2$ was prepared by the literature method.[11a] The oxo−aryl complexes (HBpz$_3$)ReO(Ar)(Cl) (Ar = 3,4- or 2,4-dimethylphenyl) were prepared by photolysis of (HBpz$_3$)ReO(I)(Cl) in *o*- and *m*-xylene, respectively.[10a,73]

All triflate complexes and cationic adducts are quite water sensitive, so reactions and preparations involving them were performed under vacuum or N_2 using standard techniques. Other neutral complexes were stable to air, and no special precautions were employed in their handling.

(HBpz$_3$)ReO(Ph)$_2$. Into a three-neck 1-L round-bottom flask were placed 1.005 g of (HBpz$_3$)ReOCl$_2$ (2.07 mmol) and a stirbar. Two of the necks were stoppered, and the third was used to attach the flask to the vacuum line. Into the flask was transferred 400 mL of dry benzene. The flask was warmed to room temperature and the solution stirred to dissolve as much of the rhenium compound as possible. Under a flow of nitrogen, one of the stoppers was replaced by a rubber septum. Through the septum a slurry made by adding 5.0 mL of 1.8 M phenyllithium in cyclohexane/ether (Aldrich, 9 mmol) to a mixture of 410 mg of anhydrous $ZnCl_2$ (3.01 mmol, 1.45 equiv/Re) in 10 mL of Et_2O was syringed over the course of 10 min. The solution turned from blue to green during the addition. The solution was stirred under N_2 for 1.5 h, opened to the air, and gravity filtered to remove some brown solids. The solvent was removed on the rotary evaporator, and the residue was taken up in toluene and chromatographed in portions using Pasteur pipets filled with silica gel, eluting with toluene. The combined blue fractions from this initial chromatography were rechromatographed on pipets filled with silica, eluting first with hexane to remove biphenyl, and then with 2:1 toluene:hexane, collecting the blue material in several fractions. The fractions were checked for purity by TLC and rechromatographed as needed to achieve purity. The TLC-pure fractions were combined, crystallized from toluene/hexane, and washed with hexane to give 793 mg of (HBpz$_3$)ReO(Ph)$_2$ (67%). ^{1}H NMR: δ 5.92 (t, 1 H), 6.42 (t, 2 H), 6.75, 7.52 (d, 1 H, peak at 6.75 is obscured by the *para* protons), 7.70, 7.94 (d, 2 H), 6.75 (t, 7 Hz, 2 H, Ph *para*), 6.99 (d, 7 Hz, 4 H, Ph *ortho*), 7.31 (t, 8 Hz, 4 H, Ph *meta*). ^{13}C{^{1}H} NMR: δ 105.4, 134.8, 147.3 (pz *trans* to oxo), 107.9, 138.0, 146.7 (pz *trans* to Ph), 161.2 (*ipso*), 141.4 (*ortho*), 127.8 (*para*), 126.2 (*meta*). IR (Nujol mull): 2520 (m, ν_{BH}), 1573 (m, $\nu_{C=C}$), 1002 (s, ν_{ReO}), 894 (w), 815 (w), 791 (m), 757 (m), 736 (m), 669 (w). UV−vis (CH_3CN): λ_{max} = 660 nm (ϵ = 130 M^{-1} cm^{-1}), 345 sh (1700), 263 (1.5×10^4). FABMS: 570 (M^+). Anal. Calcd for $C_{21}H_{20}BN_6ORe$: C, 44.29; H, 3.54; N, 14.76. Found: C, 43.82; H, 3.50; N, 14.77.

(HBpz$_3$)ReO(Ph)I. Into a flask containing 493 mg of (HBpz$_3$)ReO(Ph)$_2$ (0.865 mmol) and 877 mg of iodine (3.46 mmol, 4.0 equiv) was vacuum transferred 15 mL of toluene. The solution was refluxed under nitrogen for 3.5 h, at which point TLC indicated that the material consisted predominantly of (HBpz$_3$)ReO(Ph)I, contaminated with traces of the oxo−diiodide complex and of unreacted diphenyl complex. The solution was opened to the air and added to 35 mL of fresh toluene. The toluene solution was washed twice with 40 mL of 0.5 M aqueous sodium thiosulfate and once with 40 mL of water and dried over $MgSO_4$. After stripping down to a green oil, the residue was taken up in a minimum volume of 2:1 toluene:hexane and flash chromatographed in portions on short silica gel columns (since the phenyl iodide complex decomposes appreciably on longer columns). Elution was with 2:1 toluene:hexane, and the green eluate was collected in several fractions, which were then analyzed by TLC. Pure fractions were set aside, and those contaminated by faster moving blue (HBpz$_3$)ReO(Ph)$_2$ or by slower moving yellow (HBpz$_3$)ReOI$_2$ were rechromatographed as necessary. The TLC-pure fractions were combined and recrystallized from toluene/hexane to yield 380 mg of (HBpz$_3$)ReO(Ph)I (71%). ^{1}H NMR: δ 5.88, 6.44, 6.54 (t, 1 H), 7.13, 7.41, 7.46, 7.91, 7.95, 8.77 (d, 1 H), 6.85 (t, 7 Hz, 1 H, *para*), 7.15 (d, 8 Hz, 2 H, *ortho*), 7.35 (t, 8 Hz, 2 H, *meta*). ^{13}C{^{1}H} NMR: δ 106.0, 108.5, 108.8, 134.8, 138.4, 139.4, 148.5, 149.7, 150.0 (pyrazoles), 126.1 (*meta*), 129.4 (*para*), 145.7 (*ortho*), 157.3 (*ipso*). IR (evaporated film): 2517 (m, ν_{BH}), 980 (s, ν_{ReO}), 791 (m), 735 (m), 698 (w), 668 (w). FABMS: 620, 621 (M^+, $M + H^+$). Anal. Calcd for $C_{15}H_{15}BN_6IORe$: C, 29.09; H, 2.44; N, 13.57. Found: C, 29.49; H, 2.52; N, 13.44.

(HBpz$_3$)ReO(Ph)(OTf). Into a 25-mL round-bottom flask were placed 149.5 mg of (HBpz$_3$)ReO(Ph)I (0.241 mmol), 71.4 mg of AgOTf (0.278 mmol, 1.15 equiv), and a magnetic stirbar. The flask was attached to a swivel-frit assembly, evacuated on the vacuum line, and 12 mL of dry toluene vacuum transferred into it. The mixture was warmed to room temperature, giving a green solution with dark green solids. The flask was wrapped in aluminum foil to protect it from light and allowed to stir at room temperature in vacuo for 2 days. The blue solution was filtered away from the yellow precipitate of AgI, and the volume of toluene reduced to ca. 1 mL. At −78 °C 20 mL of pentane was vacuum transferred on top of the solution and the mixture allowed to warm temperature and to stand overnight. The precipitated blue solid was filtered, washed with pentane, and dried in vacuo for 1.5 h. The yield of (HBpz$_3$)ReO(Ph)(OTf) was 142.5 mg (92%). ^{1}H NMR: δ 6.02, 6.49, 6.57 (t, 1 H), 7.12, 7.35, 7.58, 7.91, 7.97, 8.42 (d, 1H), 7.04 (tt, 7, 1 Hz, 1 H; *para*), 7.10 (dd, 8, 1 Hz, 2 H, *ortho*), 7.44 (t, 8 Hz, 2 H, *meta*). ^{13}C{^{1}H} NMR: δ 106.4, 108.5, 109.7, 135.8, 138.4, 141.5, 146.9, 148.5, 150.4 (pzs), 126.4 (*meta*), 130.9 (*para*), 143.6 (*ortho*), 159.2 (*ipso*), *C*F_3SO_3 not observed. ^{19}F NMR: δ −0.63 (s). IR (Nujol mull): 2524 (m, ν_{BH}), 1350 (s), 1236 (s), 1192 (s), 1161 (m, ν_{CF3SO3}), 990 (s), 976 (s, ν_{ReO}), 784 (m), 738 (m), 722 (w), 630 (m). MS: 642 (M^+).

(71) Gordon, A. J.; Ford, R. A. *The Chemist's Companion*; John Wiley and Sons: New York, 1972; p 303.

(72) Fenselau, A. H.; Moffat, J. G. *J. Am. Chem. Soc.* **1966**, *88*, 1762−1765.

(73) Brown, S. N. Ph.D. Thesis, University of Washington, Seattle, WA, 1994; Chapter 2.

(HBpz$_3$)ReO(OTf)$_2$. Into a large glass bomb with a stirbar and a Teflon valve were loaded 575 mg of (HBpz$_3$)ReOCl$_2$ (1.18 mmol) and, in the drybox, 714 mg of AgOTf (2.78 mmol, 2.36 equiv). The bomb was evacuated, and 40 mL of dry CH_2Cl_2 was vacuum transferred in. The valve was closed and the solution heated at 85 °C for 5 h, at which point the solution was deep blue with a pale violet precipitate. The solution was filtered through a plug of glass wool in the drybox and then placed in a flask on a swivel-frit apparatus. The dichloromethane was removed on the vacuum line and replaced with 45 mL of toluene. The toluene solution was filtered through the swivel frit, its volume was reduced to 10 mL, and 25 mL of pentane was transferred in on top of the toluene solution. After the layers were allowed to come to room temperature and mix overnight, the precipitated blue solids were filtered, washed with fresh pentane, and dried in vacuo. Yield: 260 mg (31%). ^{1}H NMR: δ 6.25 (t, 1 H), 6.66 (t, 2 H), 7.64, 7.85 (d, 1 H), 8.03, 8.14 (d, 2 H). ^{13}C{^{1}H} NMR: δ 110.3, 141.7, 150.4 (pz *trans* to O_3SCF_3), 107.4, 137.4, 147.0 (pz *trans* to oxo), *C*F_3SO_3 not observed. ^{19}F NMR: δ 2.43 (s). IR (Nujol mull): 2536 (ν_{BH}), 1516, 1357, 1242, 1200, 1148 (ν_{CF3SO3}), 960, 938 (ν_{ReO}), 789, 670. MS: 714 (M^+). Anal. Calcd for $C_{11}H_{10}BF_6N_6S_2O_7Re$: C, 18.52; H, 1.41; N, 11.78. Found: C, 18.98; H, 1.53; N, 11.70.

[(HBpz$_3$)ReO(Ph)(OSMe$_2$)]OTf is formed in solution on addition of Me_2SO to (HBpz$_3$)ReO(Ph)(OTf) in the presence of Me_2S. ^{1}H NMR: δ 6.11, 6.48, 6.65 (t, 1 H), 7.05, 7.41, 7.61, 7.99, 8.00, 8.26 (d, 1 H), 6.98 (d, 7 Hz, 2 H, *ortho*), 7.04 (t, 7 Hz, 1 H, *para*), 7.47 (t, 8 Hz, 2 H, *meta*), 3.12, 3.23 (s, 3 H each, Re-OS(C*H*$_3$)(C*H*′$_3$)). IR ($CHCl_3$ solution, formed by adding (HBpz$_3$)ReO(Ph)(OTf) to a solution of excess Me_2S and Me_2SO in $CHCl_3$ and subtracting a background of the ligand solution): 2520 (m, ν_{BH}), 1276 (vs), 1164 (s), 1030 (vs, ionic $CF_3SO_3^-$), 985 (s, $\nu_{Re=O}$); 858 (s, br, ν_{S-O}), 638 (s), 574 (w), 518 (m). If the complex is synthesized using an excess of ^{18}O-enriched Me_2SO ($\nu_{S-^{18}O}$ = 1013 cm^{-1}, calcd 1015 cm^{-1}), two new bands are observed; the oxo stretch is shifted to 948 cm^{-1} (calcd for Re−^{18}O 933 cm^{-1}) and the S−O stretch to 826 cm^{-1} (calcd for S−^{18}O 826 cm^{-1}).

Other adducts which may be formed by addition of the appropriate ligand to dichloromethane solutions of (HBpz$_3$)ReO(Ph)(OTf) include the following: **[(HBpz$_3$)ReO(Ph)(py)]OTf.** ^{1}H NMR: δ 6.21, 6.54, 6.66 (t, 1 H), 6.76, 7.45, 7.64, 7.80, 8.08, 8.12 (d, 1 H), 6.82 (dd, 8, 1 Hz, 2 H, *o*-Ph), 6.90 (tt, 7, 1 Hz, 1 H, *p*-Ph), 7.50 (t, 8 Hz, 2 H, *m*-Ph), 7.94 (ddd, 7, 5, 1 Hz, 2 H, py 3,5-H), 8.11 (1 H, obscured by pz protons, py 4-H), 8.48 (d, 5 Hz, 2 H, py 2,6-H). **[(HBpz$_3$)ReO(Ph)(SMe$_2$)]OTf** is formed in equilibrium with (HBpz$_3$)ReO(Ph)(OTf) in the presence of a large excess of dimethyl sulfide. ^{1}H NMR: δ 6.32, 6.49, 6.71 (t, 1 H), 7.46, 7.54, 7.77, 7.98, 8.12, 8.36 (d, 1 H), 6.60 (dd, 7, 1 Hz, 2 H, *ortho*), 6.84 (tt, 7, 1 Hz, 1 H, *para*), 7.49 (t, 8 Hz, 2 H, *meta*), 3.08 (s, 6 H, ReS(C*H*$_3$)$_2$).

(HBpz$_3$)ReO(OPh)$_2$. Into a glass reaction vessel with a Teflon valve were placed 352.8 mg of (HBpz$_3$)ReOCl$_2$ (0.726 mmol), 218 mg of phenol (2.32 mmol), and a magnetic stirbar. The vessel was evacuated, and 30 mL of dry acetonitrile and 0.7 mL dry triethylamine were vacuum transferred into it. The solution was heated in vacuo at 80 °C for 2 days. The vessel was then filled with N_2 and, under a flow of N_2, 720 mg more of phenol (7.65 mmol) was added. The solution was freeze−pump−thaw degassed and heated, with stirring, at 80 °C for 3 more days. The reaction vessel was opened to the air, its contents were poured into a round-bottom flask, and the volatiles were removed on a rotary evaporator. The residue was dissolved in toluene and the toluene solution washed twice with 50 mL of aqueous KOH (0.18 M). The green organic layer was dried over $MgSO_4$, its volume reduced to a minimum, and then the layer loaded onto a silica gel column. Elution with dichloromethane separated the dark green (HBpz$_3$)ReO(OPh)$_2$ from a faster-moving green band containing (HBpz$_3$)ReOCl$_2$ and (HBpz$_3$)ReO(OPh)Cl. The chromatographically pure material was crystallized from hexane, filtered, washed with 5 mL of hexamethyldisiloxane, and air-dried to yield 196 mg of (HBpz$_3$)ReO(OPh)$_2$ (45%) as a green powder. ^{1}H NMR: δ 6.18 (t, 1 H), 6.30 (t, 2 H), 7.58, 7.84 (d, 1 H); 7.37, 7.83 (d, 2 H), 6.60 (d, 7 Hz, 4 H, *ortho*), 6.78 (t, 7 Hz, 2 H, *para*), 7.20 (t, 7 Hz, 4 H, *meta*). ^{13}C{^{1}H} NMR: δ 107.9, 138.8, 148.3 (pz *trans* to OPh), 106.1, 135.1, 144.1 (pz *trans* to oxo), 176.2 (*ipso*), 128.8 (*meta*), 121.0 (*para*), 120.0 (*ortho*). MS: 602 (M^+). IR (Nujol mull): 2502 (m, ν_{BH}), 1588, 1482 (s, $\nu_{C=C}$), 1240, 1223 (s, ν_{CO}), 1161 (m), 966 (s, $\nu_{Re=O}$), 920 (w), 891 (w), 850 (s), 791 (w), 693 (m). Anal. Calcd for $C_{21}H_{20}BN_6O_3Re$: C, 41.94; H, 3.35; N, 13.97. Found: C, 41.82; H, 3.37; N, 13.93.

(HBpz$_3$)ReO(OPh)(OTf). A sample of (HBpz$_3$)ReO(OPh)$_2$ (90.3 mg, 0.150 mmol) was weighed into a small glass vial and taken into the drybox. In the drybox were added 3 mL of C_6H_6 and 32.5 μL of trimethylsilyl triflate (0.168 mmol, 1.12 equiv). The vial was capped and allowed to stand at room temperature for 2 h. At this point the vial was placed inside a larger jar with 15 mL of pentane and the pentane vapor allowed to diffuse into the benzene solution overnight to produce a green gum. The liquid was decanted off the gum and discarded. The gum was extracted with 30 mL of hot heptane, the green heptane solution allowed to cool, and the olive-green product filtered off and washed with a small amount of pentane to yield 10.0 mg of the phenoxy triflate complex. This procedure left a large amount of the original gum undissolved. To extract more product, the gum was dissolved in 1 mL of benzene and then 15 mL of hot heptane added to the solution, which precipitated a brownish-green oily material. The solution was decanted away from the oil, the benzene/heptane addition sequence repeated, and the solution combined with the first extract. A red-brown oil remained and was discarded. The combined benzene/heptane solution was cooled at −20 °C for 4 h, filtered, and washed twice with 5 mL of pentane to yield 44.0 mg of olive-green solid; the total yield of (HBpz$_3$)ReO(OPh)(OTf) was 54.0 mg (55%). ^{1}H NMR: δ 6.24, 6.41, 6.53 (t, 1 H), 7.32, 7.62, 7.82, 7.84, 7.99, 8.24 (d, 1 H), 6.51 (d, 8 Hz, 2 H, *ortho*), 6.87 (tt, 7, 1 Hz, 1 H, *para*), 7.26 (dd, 8, 7 Hz, 2 H, *meta*). ^{13}C{^{1}H} NMR ($CDCl_3$): δ 106.4, 108.2, 109.0, 135.5, 138.0, 140.8, 144.8, 148.8, 149.6 (pzs), 174.8 (*ipso*), 128.8 (*meta*), 122.3 (*para*), 118.9 (*ortho*). ^{19}F NMR: δ −0.59 (s). IR (Nujol mull): 2524 (m, ν_{BH}), 1588, 1483 (m, $\nu_{C=C}$), 1353 (s), 1239 (m), 1198 (s), 1161 (m) (CF_3SO_3), 975 (s, ν_{ReO}), 856 (m), 694 (m). MS: 658 (M^+), 565 (M^+ − OPh), 508 (M^+ − HOTf), 432 ([HBpz$_3$]ReO$_2^+$).

Adducts that form when the appropriate ligand is added to solutions of (HBpz$_3$)ReO(OPh)(OTf) in dichloromethane include the following: **[(HBpz$_3$)ReO(OPh)(py)]OTf.** ^{1}H NMR: δ 6.25, 6.30, 6.68 (t, 1 H), 6.86, 7.16, 7.86, 8.03 (d, 1 H), 7.96 (d, 2 H, two superimposed pz doublets), 6.26 (d, 7 Hz, 2 H, *o*-OPh), 6.91 (t, 7 Hz, 1 H, *p*-OPh), 7.19 (t, 8 Hz, 2 H, *m*-OPh), 7.96 (t, 7 Hz, 2 H, py 3,5-H), 8.35 (t, 8 Hz, 1 H, py 4-H), 8.72 (d, 5 Hz, 2 H, py 2,6-H). **[(HBpz$_3$)ReO(OPh)(OSMe$_2$)]OTf.** ^{1}H NMR: δ 6.24, 6.27, 6.58 (t, 1 H), 6.88, 7.64, 7.77, 7.92, 7.94, 8.08 (d, 1 H), 6.42 (d, 8 Hz, 2 H, *ortho*), 6.94 (tt, 7, 1 Hz, 1 H, *para*), 7.19 (dd, 8, 7 Hz, 2 H, *meta*), 3.43, 3.48 (s, 3 H each, Re−OS(C*H*$_3$)(C*H*′$_3$)).

(HBpz$_3$)ReO(O$_2$C$_6$H$_4$). On the benchtop, 117.3 mg of (HBpz$_3$)ReOCl$_2$ (0.241 mmol) and 76.1 mg of catechol (0.691 mmol, 2.9 equiv) were placed in a 50-mL round-bottom flask with a magnetic stirring bar. Acetonitrile (25 mL) was added to dissolve the compounds, followed by 0.20 mL of triethylamine. The mixture was refluxed in the air for 22 h then allowed to cool to room temperature. After the mixture stood at room temperature for 3 h, the precipitated brown solids were isolated by suction filtration. Washing twice with both 10 mL of CH_3CN and 20 mL of Et_2O and air-drying for 20 min gave 51.8 mg of the brown catecholate complex (41%). ^{1}H NMR ($CDCl_3$): δ 5.88 (t, 1 H), 6.47 (t, 2 H), 7.25, 7.36 (d, 1 H), 7.90, 8.07 (d, 2 H), 6.83, 7.25 (m, 2 H each, catecholate protons). ^{13}C{^{1}H} NMR ($CDCl_3$): δ 105.8, 134.5, 140.1 (pz *trans* to oxo), 108.4, 138.8, 148.3 (pz *trans* to catecholate), 115.0, 121.7 (catecholate *C*−H), 166.2 (catecholate *C*−O). IR (Nujol mull): 3147 (w, ν_{C-H}), 2496 (m, ν_{BH}), 1238 (s, ν_{C-O}), 967 (s, ν_{ReO}), 920 (w), 895 (w), 860 (w), 803 (s), 792 (m), 748 (s), 682 (m), 660 (m). MS: 524 (M^+). Anal. Calcd for $C_{15}H_{14}BN_6O_3Re$: C, 34.43; H, 2.70; N, 16.06. Found: C, 34.35; H, 2.75; N, 16.02.

(HBpz$_3$)ReO(3,4-Me$_2$C$_6$H$_3$)(OTf) is generated in solution by heating a sealed tube containing a CD_2Cl_2 solution of (HBpz$_3$)ReO(3,4-$Me_2C_6H_3$)(Cl) with 1.13 equiv of silver triflate for 7 h at 70 °C. The reaction is quantitative by ^{1}H NMR. The triflate complex can be isolated as a fluffy green powder by filtering the dichloromethane solution through a glass frit, adding benzene, reducing the volume on the vacuum line, and carefully lyophilizing to remove the remaining benzene, but this procedure introduces substantial amounts of impurities. ^{1}H NMR: δ 6.00, 6.48, 6.56 (t, 1H), 7.10, 7.36, 7.56, 7.90, 7.95, 8.42 (d, 1H), 6.80 (dd, 8, 1 Hz, 1 H, H-6), 7.02 (br s, 1 H, H-2), 7.19 (d, 7 Hz, 1 H, H-5), 2.10 (s, 3 H, 3-C*H*$_3$), 2.55 (s, 3 H, 4-C*H*$_3$). ^{13}C{^{1}H}

NMR: δ 106.3, 108.4, 109.6; 135.7, 138.3, 141.5; 144.9, 147.1, 148.6 (pzs), 126.8 (C-5), 134.7, 140.6 (C-3, C-4), 141.0, 150.4 (C-2, C-6), 157.4 (C-1), 19.3, 20.1 (Ar−*C*H$_3$). ^{19}F NMR: δ −0.33 (s). MS: 670 (M$^+$). **(HBpz$_3$)ReO(2,4-Me$_2$C$_6$H$_3$)(OTf)** may be prepared analogously (2.4 equiv of AgOTf, C_6D_6, standing overnight and heating for 1.5 h at 80 °C). ^{1}H NMR (C_6D_6): δ 5.39, 5.49, 5.81 (t, 1 H), 6.78, 6.79, 6.95, 7.07, 7.38, 8.71 (d, 1 H), 6.27 (br, 1 H, 6-H), 6.83 (br d, $J \approx 7$ Hz, 1 H, 5-H), 7.48 (s, 1 H, 3-H), 3.37 (br s, 3 H, 2-C*H*$_3$), 2.52 (s, 3 H, 4-C*H*$_3$).

Oxidation of (HBpz$_3$)ReO(3,4-Me$_2$C$_6$H$_3$)(OTf). (a) With Pyridine *N*-Oxide. A solution of (HBpz$_3$)ReO(3,4-Me$_2$C$_6$H$_3$)(OTf) in CD_2Cl_2, prepared as described above, was filtered through a glass frit in the drybox to remove silver chloride and unreacted silver triflate. To the solution was added an excess of pyridine *N*-oxide (∼4 equiv), causing the solution to turn immediately from green to dark red and then gradually to reddish-brown. The solution was rapidly taken out of the drybox and chilled in a dry ice−acetone bath (time of reaction at room temperature = 2 min). NMR spectra at low temperature indicated that the reaction was complete, the only diamagnetic products being a mixture of two catecholate complexes (35% yield) and (HBpz$_3$)ReO$_3$ (12% yield); there are also broad signals outside the diamagnetic region. The solution was warmed to room temperature, exposed to air, and promptly chromatographed on silica gel, eluting with CH_2Cl_2. The colored fraction contained the catecholate complexes, the trioxo complex, and some paramagnetic material. The symmetric (HBpz$_3$)ReO(4,5-Me$_2$C$_6$H$_2$O$_2$) and unsymmetric (HBpz$_3$)ReO(3,4-Me$_2$C$_6$H$_2$O$_2$) are formed in a 3.3:1 ratio. ^{1}H NMR (4,5-Me$_2$ isomer): δ 5.90 (t, 1 H), 6.51 (t, 2 H), 7.18, 7.44 (d, 1 H), 7.97, 8.02 (d, 2 H), 6.99 (s, 2 H, 3- and 6-H, catecholate), 2.29 (s, 6 H, 4- and 5-C*H*$_3$). ^{1}H NMR (3,4-Me$_2$ isomer): δ 5.91, 6.51, 6.53 (t, 1 H), 7.17, 7.44, 7.97, 8.00, 8.02, 8.07 (d, 1 H), 6.64, 6.94 (d, 8 Hz, 1 H each, 5-H and 6-H, catecholate), 2.29, 2.33 (s, 3 H each, 3- and 4-C*H*$_3$). MS (mixture of isomers): 552 (M$^+$).

Oxidation of (HBpz$_3$)ReO(3,4-Me$_2$C$_6$H$_3$)(OTf). (b) With Dimethyl Sulfoxide. Addition of Me$_2$SO to a solution of (HBpz$_3$)ReO(3,4-Me$_2$C$_6$H$_3$)(OTf), prepared as in (a), immediately produces [(HBpz$_3$)ReO(3,4-Me$_2$C$_6$H$_3$)(OSMe$_2$)]OTf. ^{1}H NMR: δ 6.10, 6.47, 6.64 (t, 1 H), 7.07, 7.41, 7.60, 7.99, 8.00, 8.22 (d, 1 H), 6.64 (obscured by pz, 1 H, 6-H), 6.88 (s, 1 H, 2-H), 7.23 (d, 7 Hz, 1 H, 5-H), 3.16, 3.19 (sl br s, 3 H each, ReOS(C*H*$_3$)(C*H*′$_3$)), 2.61 (s, 3 H, 4-C*H*$_3$), 2.10 (s, 3 H, 3-C*H*$_3$). A new rhenium species, the phenoxide complex [(HBpz$_3$)ReO(O-3,4-Me$_2$C$_6$H$_3$)(OSMe$_2$)]OTf, slowly grows in intensity at the expense of the aryl complex. ^{1}H NMR: δ 6.25 (t, 2 H, two superimposed pz signals), 6.58 (t, 1 H), 6.93, 7.64, 7.74, 7.91, 7.95, 8.07 (d, 1 H), 6.03 (dd, 8, 3 Hz, 1 H, 6-H), 6.29 (d, 3 Hz, 1 H, 2-H), 6.89 (d, 8 Hz, 1 H, 5-H), 3.41, 3.46 (s, 3 H each, ReOS(C*H*$_3$)(C*H*′$_3$)), 2.21 (s, 3 H, 3- or 4-C*H*$_3$, other signal is obscured, probably by Me$_2$S at 2.10 ppm).

Oxidation of (HBpz$_3$)ReO(2,4-Me$_2$C$_6$H$_3$)(OTf) with Pyridine *N*-Oxide. The C_6D_6 solution of (HBpz$_3$)ReO(2,4-Me$_2$C$_6$H$_3$)(OTf) prepared as described above was filtered through a glass frit in the drybox and the frit washed with a small portion of fresh C_6H_6. The benzene solution was evaporated on the vacuum line and the residue taken up in CD_2Cl_2. The methylene chloride solution was poured onto 1.6 equiv of pyridine *N*-oxide in an NMR tube and the tube sealed and allowed to stand overnight. In the drybox it was then broken open and an excess of Me$_4$NCl added. This mixture was sealed in an NMR tube and allowed to stand for 3 days at room temperature. NMR showed the formation of (HBpz$_3$)ReO(O-2,4-Me$_2$C$_6$H$_3$)Cl as well as some of the chloride complex derived from unreacted aryl (HBpz$_3$)ReO(2,4-Me$_2$C$_6$H$_3$)Cl; the catecholate complex (HBpz$_3$)ReO(3,5-Me$_2$C$_6$H$_2$O$_2$) and the trioxo complex (HBpz$_3$)ReO$_3$ also were present (as they were before addition of chloride). The tube was then broken open and the solution chromatographed on silica gel. Elution with toluene gave the aryloxy chloride complex **(HBpz$_3$)ReO(O-2,4-Me$_2$C$_6$H$_3$)Cl**, contaminated with aryl chloride complex. ^{1}H NMR: δ 6.05, 6.50, 6.54 (t, 1 H), 7.46, 7.60, 7.82, 7.89, 7.99, 8.01 (d, 1 H), 6.51 (d, 8 Hz, 1 H, 6-H), 7.01 (dd, 8, 1 Hz; 5-H), 7.06 (d, 1 Hz, 1 H, 3-H), 2.23, 2.44 (s, 3 H each, 2- and 4-C*H*$_3$). MS: 572 (M$^+$), 536 (M$^+$ − HCl). Elution with methylene chloride gave the catecholate complex **(HBpz$_3$)ReO(3,5-Me$_2$C$_6$H$_2$O$_2$)**, contaminated with (HBpz$_3$)ReO$_3$; only the 3,5-isomer is observed. ^{1}H NMR: δ 5.91, 6.51, 6.53 (t, 1 H), 7.18, 7.44, 7.97, 8.00, 8.02, 8.05 (d, 1 H), 6.51 (obscured by pz t, 1 H, 4- or 6-H), 6.86 (d, 1 Hz, 1 H, 6- or 4-H), 2.32, 2.35 (s, 3 H each, 3- and 5-C*H*$_3$). MS: 552 (M$^+$).

Pyridine *N*-oxide-*d*$_5$ was prepared to allow generation of [(HBpz$_3$)ReO$_2$(Ph)]OTf without extraneous peaks in the aromatic region of the ^{1}H NMR. It was prepared according to the literature procedure used previously for other labeled pyridine *N*-oxides.[74] Pyridine-*d*$_5$ (Cambridge Isotope Laboratories, 338 mg, 4.02 mL) was mixed with 1.3 mL of glacial acetic acid and 0.5 mL of 30% H_2O_2, and the mixture was heated at 75 °C overnight. Since the method of purification given failed to produce pure material, the crude material (after evaporation of the volatiles on a rotary evaporator) was treated as described by Ochiai.[75] Sodium carbonate was added until the mixture was distinctly basic, the slurry was extracted with chloroform, and the chloroform was dried over Na_2SO_4. After the chloroform was stripped down, the white residue was sublimed in vacuum to give 49.4 mg of C_5D_5NO (12%), which was stored in the drybox. MS: 100 (M$^+$), from the intensity of the *m*/*z* = 99 peak (1.1%), the compound is estimated to be 99.8% D. Mp (sealed capillary): 65.5−66 °C (uncor).

Exchange Kinetics of [(HBpz$_3$)ReO(Ph)(OS[CD$_3$]$_2$)]OTf with (CH$_3$)$_2$S. Samples were prepared by adding an excess of $(CD_3)_2SO$ (2 equiv) to solutions of (HBpz$_3$)ReO(Ph)(OTf) in CD_2Cl_2 at room temperature in the drybox. The mixtures were then placed in NMR tubes sealed to ground-glass joints and attached to calibrated gas addition bulbs. The tubes were affixed to the vacuum line, chilled in dry ice−acetone baths, and degassed at this temperature. Then, at liquid nitrogen temperature, a known quantity of $(CH_3)_2S$ was added by vacuum transfer, using the calibrated bulb and observed pressure. Me$_4$Si was also added as an internal standard. The tubes were sealed while cooled in liquid nitrogen and were thawed and mixed at −78 °C immediately before being inserted into the precooled probe of the NMR spectrometer. Spectra were taken, monitoring the growth of the ReOS(C*H*$_3$)$_2$ signals as a function of time. After isotope exchange was judged to be complete, the sample was allowed to stand for a few minutes at 246 K to ensure complete equilibration. The [Re]/[Me$_2$S] ratio was measured by NMR at this point from the ratio of the integrals Re−OS(C*H*$_3$)$_2$/(C*H*$_3$)$_2$S. (The apparent initial ratio cannot be used since a significant amount of $(CD_3)_2S$ is produced from the $(CD_3)_2SO$ in the few minutes that the sample is at room temperature.)

Magnetization transfer in [(HBpz$_3$)ReO(Ph)(OSMe$_2$)]OTf was performed on solutions containing a large (>20 equiv) excess of free dimethyl sulfide. The (C*H*$_3$)$_2$S peak at 2.10 ppm was selectively inverted using a DANTE pulse sequence, and the resulting FID (acquired after the desired delay) was subtracted from an FID acquired in an analogous manner but with inversion carried out well off-resonance. The difference spectra therefore show positive peaks whose magnitude is proportional to the nonequilibrium magnetization of the relevant signals. Analysis of the growth of the [(HBpz$_3$)ReO(Ph)(OS(C*H*$_3$)$_2$)]OTf signals is complicated by differential relaxation of free Me$_2$S and bound Me$_2$SO. This concern was circumvented by formulating the kinetic expression in terms of M_{eq}, the steady-state ratio of the nonequilibrium magnetizations of Re−OS(C*H*$_3$)$_2$ and S(C*H*$_3$)$_2$, which is achieved after about 5 half-lives or so. The derivation of eq 19 is

$$k = M_{eq}([Me_2S]/[Re])k_{obs} \quad (19)$$

given in the Supporting Information. The ratio of concentrations was measured from normal NMR spectra taken before and after the magnetization transfer experiment, and the ratios were averaged. k_{obs} was determined from a plot of $\ln(M_{eq} - M_t)$ vs time. Corrections for differential relaxation were <20% at or above room temperature, but were substantial below room temperature (e.g., $k = 3.4k_{obs}$ at 277 K).

Reaction Kinetics of [(HBpz$_3$)ReO(Ph)(OSMe$_2$)]OTf. A weighed amount of (HBpz$_3$)ReO(Ph)(OTf) was added in the drybox to a known volume of CD_2Cl_2 to which some Me$_2$S had been added on the vacuum line (to slow the initial reaction with Me$_2$SO). Me$_2$SO was added to this solution to generate [(HBpz$_3$)ReO(Ph)(OSMe$_2$)]OTf, and (Me$_3$Si)$_2$O was added as an internal standard. This stock solution was divided into portions in NMR tubes sealed to ground glass joints, additional

(74) Snerling, O.; Nielsen, C. J.; Nygaard, L.; Pedersen, E. J.; Sørensen, G. O. *J. Mol. Struct.* **1975**, *27*, 205−211.
(75) Ochiai, E. *J. Org. Chem.* **1953**, *18*, 534−551.

Me_2SO or $(HBpz_3)ReO(Ph)(OTf)$ was added if desired, and the tubes were capped with Teflon needle valves. The NMR tube assemblies were taken out to the vacuum line, cooled to −78 °C, and evacuated. Additional Me_2S was condensed into the tubes if desired, and the tubes were sealed with a torch. The sealed NMR tubes were kept at −78 °C until reaction monitoring by ^1H NMR began.

Concentrations of species were determined by integration of the ^1H NMR signals of $[(HBpz_3)ReO(Ph)(OS[CH_3]_2)]OTf$, $[(HBpz_3)ReO(OPh)(OS[CH_3]_2)]OTf$, and $(CH_3)_2SO_2$ with respect to internal $(Me_3Si)_2O$. Data were taken over the initial portion of the reaction (10−20% decrease in the concentrations of $[(HBpz_3)ReO(Ph)(OSMe_2)]OTf$ and free Me_2SO), and rates were determined from the slope of concentration vs time plots during this period. No significant curvature of these plots was observed. For reactions performed above room temperature, tubes were completely immersed in a stirred water bath in a large Dewar flask kept at constant temperature by circulating water from a recirculating bath through a copper coil in the Dewar. After a given interval in the water bath, the tubes were removed, immediately plunged into a beaker of room temperature water, and analyzed by ^1H NMR at room temperature. The tubes were then reintroduced into the water bath for a second interval, and so on. The time the samples spent at room temperature was recorded, and data were corrected for the reaction that took place at room temperature.

Phenyl-to-Oxo Migration Kinetics of $[(HBpz_3)ReO_2(Ph)]OTf$. A typical sample was prepared by loading solid $(HBpz_3)ReO(Ph)(OTf)$ and C_5H_5NO into an NMR tube sealed to a ground-glass joint in the drybox. The tube was attached to a needle valve and promptly taken out to the vacuum line and cooled in a dry ice−acetone bath. Little reaction appears to take place in the solid state. The tube was evacuated and CD_2Cl_2 slowly vacuum transferred onto the solid, keeping the tube cold. After a small amount of Me_4Si was transferred as an internal standard, the tube was sealed with a torch. The solution was mixed while immersed in dry ice−acetone by repeatedly inverting until all the solids had dissolved. The deep orange solution was then kept in the dry ice−acetone bath until ready to use. It was taken out of the bath and promptly inserted into an NMR probe precooled to the temperature desired for kinetic measurement. The temperature generally stabilized within 5 min, and spectra were then acquired periodically, using a 40-s relaxation delay to ensure accurate integration. Integrals of the products $(HBpz_3)ReO(O_2C_6H_4)$, $[(HBpz_3)ReO(OPh)(py)]OTf$, and $(HBpz_3)ReO(OPh)(Cl)$ were measured using the peaks in the 5.7−6.7 ppm region. Me_4Si or the methyl peak of residual toluene from the phenyl triflate complex was used as internal standard. To get t_∞ values for the total amount of products, the tube was warmed to 285 K after the reaction had essentially finished and was allowed to stand at this temperature for about 0.5 h; final concentrations of the product were then measured by NMR. The total amount of the three phenyl oxidation products at any given time were added together and $\ln(\text{products}_\infty - \text{products}_t)$ was plotted against time to give the first-order rate constants.

X-ray Crystallography of $(HBpz_3)ReO(OTf)_2 \cdot C_6D_6$. Large single crystals of the bis(triflate) complex $(HBpz_3)ReO(OTf)_2$ were grown by allowing a supersaturated solution of the compound in benzene-d_6 (10 mg in 0.5 mL) to stand at room temperature for 6 months in a sealed NMR tube under vacuum. This procedure allows the small crystals initially present to gradually grow in size. The tube was cracked open in the air and the supernatant poured out; the crystals were then rapidly taken into the drybox, where several were mounted inside glass capillaries. The capillaries were sealed with a torch, and one containing a deep blue crystal 0.2 × 0.25 × 0.35 mm was mounted on the CAD4 diffractometer. For details of data collection, see Table 1. Decay was less than 1% during acquisition and was ignored in data reduction; other details of data reduction are as described elsewhere.[11a] The rhenium atoms were located without difficulty from a Patterson map and refinement proceeded smoothly to $R = 4.76\%$, $R_w = 6.57\%$, and goodness of fit = 1.22.

Acknowledgment. We thank Drs. Keith Hall and David Barnhart for their assistance with the X-ray crystallography and Darin D. DuMez for preparing the ^{18}O-enriched dimethyl sulfoxide. We are grateful to the National Science Foundation for financial support. S.N.B. acknowledges a National Science Foundation Predoctoral Fellowship, a Shell Graduate Fellowship, and a Howard J. Ringold Fellowship of the University of Washington Department of Chemistry.

Supporting Information Available: Derivations of kinetic equations (4) and (19), and tables of atomic positional and thermal parameters, and bond distances and angles for $(HBpz_3)ReO(OTf)_2$ (9 pages). See any current masthead page for ordering and Internet access instructions.

JA962087N